PCP
PLANT & CELL PHYSIOLOGY

Genome-Wide Profiling of Circular RNAs in the Rapidly Growing Shoots of Moso Bamboo (*Phyllostachys edulis*)

Yongsheng Wang[1,4], Yubang Gao[1,4], Hangxiao Zhang[1,4], Huihui Wang[2], Xuqing Liu[2], Xi Xu[1], Zeyu Zhang[2], Markus V. Kohnen[1], Kaiqiang Hu[1], Huiyuan Wang[2], Feihu Xi[1], Liangzhen Zhao[1], Chentao Lin[1,3] and Lianfeng Gu[1,*]

[1]College of Life Science, Basic Forestry and Proteomics Research Center, College of Forestry, Fujian Provincial Key Laboratory of Haixia Applied Plant Systems Biology, Fujian Agriculture and Forestry University, Fuzhou 350002, China
[2]College of Forestry, Fujian Agriculture and Forestry University, Fuzhou 350002, China
[3]Department of Molecular, Cell & Developmental Biology, University of California, Los Angeles, CA 90095, USA
[4]These authors contribute equally to this manuscript.
*Corresponding author: E-mail, lfgu@fafu.edu.cn; Fax, 86-591-83735305.
(Received August 27, 2018; Accepted February 24, 2019)

Circular RNAs, including circular exonic RNAs (circRNA), circular intronic RNAs (ciRNA) and exon-intron circRNAs (EIciRNAs), are a new type of noncoding RNAs. Growing shoots of moso bamboo (*Phyllostachys edulis*) represent an excellent model of fast growth and their circular RNAs have not been studied yet. To understand the potential regulation of circular RNAs, we systematically characterized circular RNAs from eight different developmental stages of rapidly growing shoots. Here, we identified 895 circular RNAs including a subset of mutually inclusive circRNA. These circular RNAs were generated from 759 corresponding parental coding genes involved in cellulose, hemicellulose and lignin biosynthetic process. Gene co-expression analysis revealed that hub genes, such as DEFECTIVE IN RNA-DIRECTED DNA METHYLATION 1 (*DRD1*), MAINTENANCE OF METHYLATION (*MOM*), dicer-like 3 (*DCL3*) and ARGONAUTE 1 (*AGO1*), were significantly enriched giving rise to circular RNAs. The expression level of these circular RNAs presented correlation with its linear counterpart according to transcriptome sequencing. Further protoplast transformation experiments indicated that overexpressing *circ-bHLH93* generating from transcription factor decreased its linear transcript. Finally, the expression profiles suggested that circular RNAs may have interplay with miRNAs to regulate their cognate linear mRNAs, which was further supported by overexpressing miRNA156 decreasing the transcript of *circ-TRF-1* and linear transcripts of *TRF-1*. Taken together, the overall profile of circular RNAs provided new insight into an unexplored category of long noncoding RNA regulation in moso bamboo.

Keywords: Circular RNAs • Hub genes • miRNAs • *Phyllostachys edulis*.

Accession numbers: High-throughput sequencing reads were deposited in the NCBI Gene Expression Omnibus (GEO) under accession number GSE104951. The bigwig tracks can be viewed at http://forestry.fafu.edu.cn/db/PhePacBio/Circular.php.

Introduction

Noncoding RNAs comprise a majority of the eukaryotic transcriptome (Djebali et al. 2012), which include long noncoding RNA (lncRNAs) and small noncoding RNAs, the latter is further classified into miRNAs, siRNAs, tRNAs and so on (Beermann et al. 2016). Circular RNAs from exon represent a class of endogenous ncRNAs and were initially reported more than 40 years ago (Sanger et al. 1976, Hsu and Coca-Prados 1979). Following these initial studies, *Sry* (Capel et al. 1993), *ANRIL* (Burd et al. 2010) and *CDR1* (Hansen et al. 2011) are well-studied circular exonic RNAs (circRNAs) to date. However, only recently genome-wide investigations based on RNA sequencing (RNA-Seq) have begun to emerge and reveal that circular RNAs are ubiquitous in eukaryotes tissues (Salzman et al. 2012), shifting the previously commonly held idea that RNA circularization is a rare event.

Circular RNAs comprise three types including circRNA that originate from back-spliced exons (Jeck and Sharpless 2014), intronic circular RNA (ciRNA) generated from lariat introns (Li et al. 2016b) and exon-intron circRNAs (EIciRNAs) localized in the nucleus to regulate the transcription of their parental gene (Li et al. 2015), respectively. A recent case study reveals that circular RNAs, such as *CDR1as* can act as a sponge for miRNAs (Hansen et al. 2013). However, the majority of circular RNAs rarely contain multiple binding sites for the same miRNAs (Guo et al. 2014). They play a role in affecting transcription and splicing (Zhang et al. 2013, Li et al. 2015), and acts as a decoy for RNA-binding proteins (Ashwal-Fluss et al. 2014). In addition, several circRNAs associated with ribosomes have a translation capacity potential (Meng et al. 2017, Pamudurti et al. 2017, Yang et al. 2017). Though circular RNAs have been investigated in plant model systems such as *Arabidopsis thaliana* (Ye et al. 2015), *Oryza sativa* (Lu et al. 2015), *Solanum lycopersicum* (Zuo et al. 2016), *Zea mays* (Chen et al. 2018) and *Gossypium* (Zhao et al. 2017), the global impact of circular RNAs in plant development remains unknown.

Previous studies using RNA-Seq investigated the regulation of gene expression at both the transcriptional and post-transcriptional levels in the fast growing shoots of moso bamboo (Peng et al. 2013a, Li et al. 2016a, Li et al. 2018). However, circular RNAs have never been reported in moso bamboo to date. In this work, we systematically investigated the expression profile of hundreds of circular RNAs in rapidly growing shoots of moso bamboo comparing eight different developmental stages using rRNA-depleted RNA-Seq libraries. Furthermore, we combined small RNA with circular RNA-Seq to identify miRNAs targeting circular RNAs, and revealed a potential regulatory network for miRNAs, circular RNAs and parental genes. Gene co-expression analysis revealed that 1,509 hub genes had a higher frequency giving rise to circular RNAs as opposed to a randomly selected 1,509 nonhub genes. This study revealed potentially regulatory circular RNAs at different stages of growing moso bamboo shoots and provided fundamental data for future research to shed light on the essential physiological roles and cellular functions of circular RNAs.

Results

Identification and characterization of circular RNAs

To identify regulatory circular RNAs at different stages of growing shoots, we constructed ribosomal (r)RNA-depleted RNA-Seq libraries for eight different developmental stages with three biological repeats, followed by Illumina HiSeq 2500 paired-end sequencing. In total, 942,189,850 million clean reads were obtained (Supplementary Table S1). In this study, we deliberately avoided a poly(A) selection method for library construction so that we could detect circular RNAs, which are nonpolyadenylated transcripts. In total, we identified 720 circRNAs generated from exon circularization, and 175 ciRNAs from lariat intron (**Fig. 1A**, full list in Supplementary Table S2). To determine whether these circular RNAs were authentic, we selected nine circRNAs for RNase R resistance experiment. Reverse Transcription-Polymerase Chain Reaction (RT-PCR) revealed that the circRNAs were resistant to the RNase R digestion (**Fig. 1B**), which confirmed the result from rRNA-depleted RNA-Seq. Transcription factor *bHLH93* (PH01000724G0700) generated circRNA and its expression was differentially regulated during eight developmental stages, which drawed our attention to this circRNA. Interestingly, circular RNAs derived from PH01000724G0700 did not show common enrichment after RNase R treatment. At first, we thought it might actually not be a bona fide circular RNAs. However, further sequencing result validated the circular RNA including back-splicing junction region. Thus we speculated that circular RNAs derived from PH01000724G0700 might be susceptible to RNase R digestion, which supports the previous finding that rare types are also found to be susceptible to this exonuclease (Jeck et al. 2013). Among these endogenous circular RNAs, the percentage for circRNA and ciRNA was approximately 80% and 20%, respectively (**Fig. 1C**). The length of circular RNAs ranged from 69 to 4,623 nt according to the back-splicing junction reads, which include precise coordinate information about the start and end. At present, there is still no efficient method to isolate circRNAs based on size. Circular RNAs were generated from the circularization of one or several adjacent exons enclosed within circular RNAs. In total, 117 out of 720 (16.25%) circRNAs originated from only one annotated exon. The remaining 603 events included two or multiple circularized exons (**Fig. 1D**). Importantly, the distribution of the number of excised exons further showed that exonic circRNA including two exons were more frequently circularized among multiple exon circularization events (**Fig. 1D**). The length of exons of single exon circularization was much longer compared to all other multiple exon circularization type (**Fig. 1E**).

Flanking inverted complementary intron sequences were reported to be involved in the biogenesis of circRNA in mammalian cells (Zhang et al. 2014, Chen 2016). However, very few inverted complementary sequences were detected around the circularized exons in moso bamboo (**Fig. 1F**). This result suggests that the biogenesis of circRNA in moso bamboo does not depend on flanking complementary sequences, which is consistent with previous findings from *Arabidopsis* (Ye et al. 2015) and *O. sativa* (Lu et al. 2015). Transposon elements (TE) corresponding to the flanking introns of circRNAs showed similar percentages in those without detectable circRNAs, suggesting that TEs may not be a major mechanism for the biogenesis of circRNA (**Fig. 1G**).

The interplay between splicing and circular RNAs

The generation of circular RNAs is dependent on the normal splicing processes by joining downstream donor sites to upstream acceptor sites (Capel et al. 1993, Zhang et al. 2014). In total, there were 291 putative splicing-related genes in moso bamboo. Interestingly, we found 10 circRNAs generated from 10 splicing-related genes (Supplementary Table S2). For example, PH01003949G0150 (KH domain-containing mRNA binding protein) and PH01005033G0050 (splicing factor 3 A subunit 3) generated circRNAs, which were resistant to RNase R (**Fig. 1B**). It has been demonstrated that the regulation of alternative splicing (AS) events depend on the AS of splicing factors themselves (Zhang et al. 2017). It will be interesting to investigate how circRNAs from these splicing factors affect the expression or splicing of their own linear transcripts.

Consistent with previous types of alternative back-splicing/splicing in circRNAs (Zhang et al. 2016), we also identified 18 alternative 5′ back-spliced circular RNA isoforms and 26 alternative 3′ back-spliced circular RNA isoforms, respectively. For example, nuclease *HARBI1* (PH01000288G0710) gave rise to three alternative circularized isoforms using alternative 5′ and 3′ back-spliced sites. Intriguingly, we identified a total of 122 circular RNAs with overlapping regions and different coordinates for back-spliced junction (**Fig. 2A**), a finding that had not been reported previously. According to the name mutually exclusive exons for linear isoforms (Pohl et al. 2013), we therefore termed them mutually inclusive circular RNAs. As an example, two circular RNAs were generated from one S-acyltransferase gene (PH01000223G0230), which had different back-splicing junction sites. However, they contained an overlapping region, as indicated in **Fig. 2A**. Next, we retrieved publicly available RNA-Seq datasets and searched them for mutually inclusive circular RNAs in other species using the same

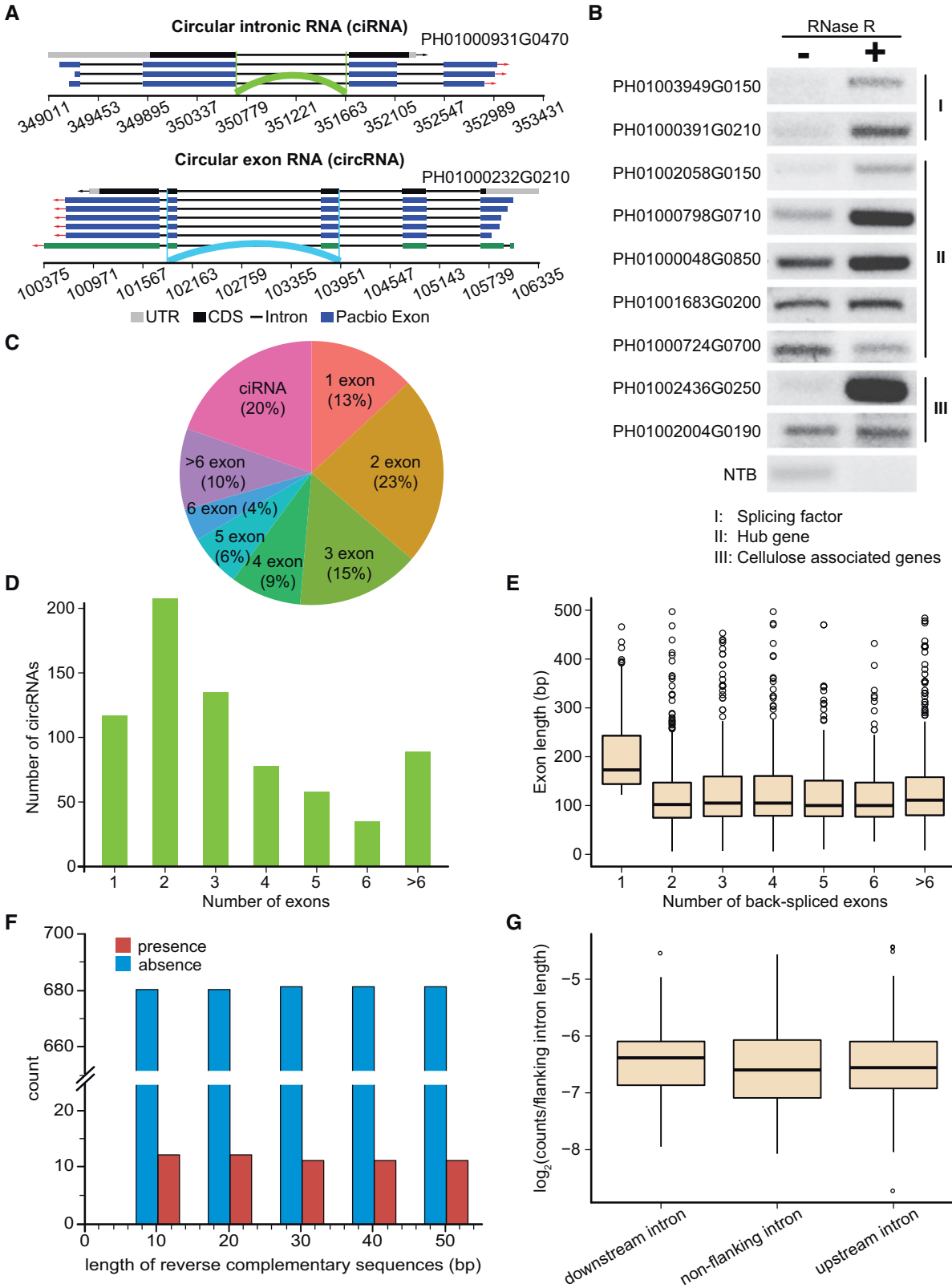

Fig. 1 Genome-wide identification and characterization of circular RNAs in moso bamboo shoots. (A) Schematic representation of ciRNA generated from the lariat intron (top panel) and circRNA (bottom panel) derived from back-splicing through the joining of 5′ donor sites and 3′ acceptor sites were indicated, respectively. (B) RT-PCR validation of circRNAs by RNase R treatment. (C) Pie chart showing the percentage of incorporated exons into circular RNAs. (D) The number of incorporated exons in circular RNAs. (E) Exon length distribution of circRNAs. (F) The number of circRNA with (red) or without (blue) inverted complementary flanking intron sequences. (G) Distribution of TE in introns flanking and nonflanking circRNAs.

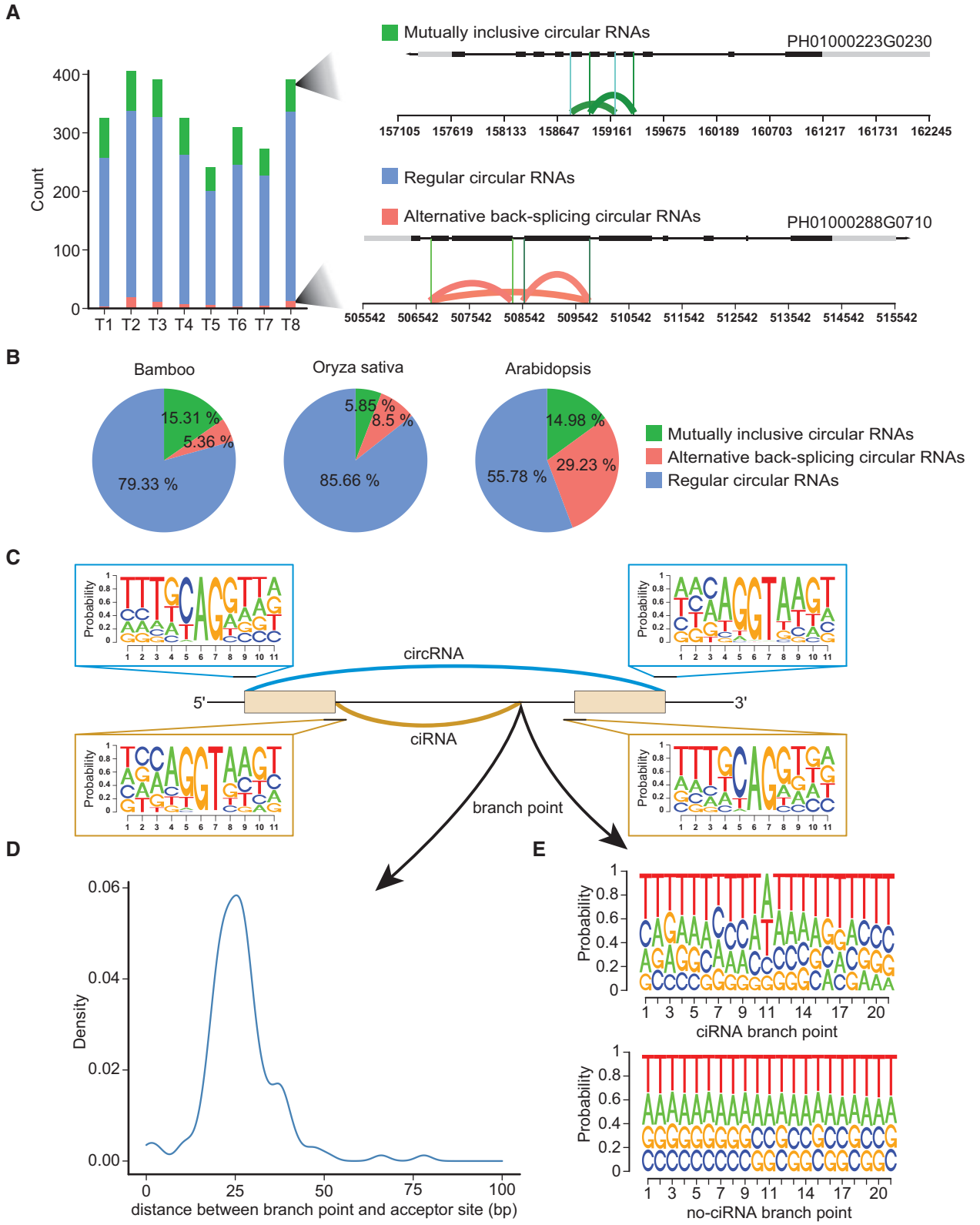

Fig. 2 Circular RNA splicing. (A) Number and structure of alternative 5′ and 3′ back-spliced circular RNA isoforms and mutually inclusive circular RNAs. (B) The percentage of mutually inclusive circular RNAs in *Arabidopsis* and *O. sativa*. (C) The sequence logo showing splicing signal around circular RNAs. (D) The distribution of the distance between branch point and acceptor sites. (E) Sequence logos presenting sequence properties around the branch point.

bioinformatics method as for our dataset. As expected, we also found mutually inclusive circular RNAs in *Arabidopsis* and *O. sativa* (**Fig. 2B**), suggesting that mutually inclusive circular RNAs were ubiquitous across different species. Though mutually inclusive circular RNA does not show any different in biogenesis which used similar back-spliced mechanisms, the presence of mutually inclusive circular RNAs and alternative back-splicing circRNAs could lead to the diversity of the circular RNAs.

To determine if circular RNAs coincided with a special splicing signal, we extracted DNA sequences from 10 nt upstream and downstream of acceptor and donor sites for ciRNA and circRNA. We found that both circRNA and ciRNA used canonical GT-AG splicing signals (**Fig. 2C**), which conclusively demonstrated that the biogenesis of circular RNAs was dependent on the spliceosome machinery. For the ciRNA, exact branch point positions could be inferred according to head-to-tail junction sites. The mean length of branch points to splicing acceptor sites for ciRNA was 25 bp (**Fig. 2D**). The sequence logo using branch points from ciRNA was different from that of non-ciRNA introns (**Fig. 2E**).

Dissecting the expression landscape of circular RNA across eight different developmental stages

In order to exclude the possibility of circular RNA being formed from as by-products of occasional high expression of linear transcripts, we firstly estimated the circular ratio of circular RNAs at 5′ donor and 3′ acceptor by comparing the number of back-spliced junction reads and the number of flanking splice junction reads for circular RNA and their linear counterparts (**Fig. 3A**). We subsequently calculated the correlation between linear transcripts and concomitant circular RNAs and observed a negative correlation (**Fig. 3B**), which suggested that circular RNAs were not a by-product of transcription. To investigate whether circular RNAs were differential expressed at differentially developmental stages, we hierarchically clustered the normalized expression levels (Supplementary Table S3). As expected, the three biological replicates were highly correlated and clustered (**Fig. 3C**). The majority of circular RNAs was supported by a few back-spliced reads (1–10) and back-spliced reads per million (RPM) mapped for most of the circular RNAs belonging to the range of 0.05–0.15 in eight different stages (**Fig. 3D, E**). Genome-wide analysis indicated that subgroups of circular RNAs were highly expressed at a specific stage during fast elongation in shoots (**Fig. 3F**). Pair-wise comparison further confirmed this trend (**Fig. 3G, H**). We randomly selected five circular RNAs for RT-PCR validation using primers spanning the back-spliced junctions, to distinguish circular RNAs from linear transcripts. Tested circular RNAs can be amplified with the expected fragment sizes consistent with our RNA-Seq results (**Fig. 4**). For instance, the single locus PH01000553G0260 gave rise to three distinct circular RNAs (**Fig. 4A**). In the future, it will be interesting to investigate multiple circularization events of high-density region.

Hub genes shown higher frequencies to generate circular RNAs

In this study, we used differentially expressed genes at different stages of shoot development to identify highly connected genes using weighted correlation network analysis (WGCNA). In total, we obtained 1,509 hub genes (Supplementary Table S4), which represented the highly interconnected genes in co-expression network and played an important role in shoot development. Among these hub genes, 84 were giving rise to circular RNAs (**Fig. 5A**). Next, we questioned whether hub genes generated significantly more circular RNA than nonhub genes. To this end, we first randomly selected 1,509 nonhub genes with similar expression levels of hub genes and detected circular RNAs derived from these genes. After repeating the process 1,000 times, we obtained the frequency of nonhub genes generating circular RNAs with a mean value and standard deviation of 53.2 and 4.26, respectively, which revealed that the simulated frequency was significantly lower ($P = 2.65^{-13}$, hypergeometric test) than observed experimental results from hub genes (**Fig. 5B**), which suggested that circRNAs derived more often from hub than nonhub genes. Compared with nonhub genes, the hub genes did not show higher expression levels ($P = 0.06$, Student's *t*-test) which indicated that the trend for hub genes to give rise to circular RNAs was not caused by by-products of transcription.

In order to exclude possible circular RNA from by-product splicing of linear transcripts, we calculated the frequency of AS events in hub gene and observed that hub gene generating circular RNAs exhibited the higher frequency of AS events than other hub genes without generating circular RNAs (**Fig 5C**). However, this does not mean that circular RNAs are a by-product of aberrant splicing. For example, splicing factors have a tendency to generate more AS events to regulate themselves and affect their function, which has been reported previous study (Chen and Cheng 2012). Similarly, hub genes display an enrichment for AS, which might be a regulator mechanism rather than a reason to generate circular RNAs. In order to validate this hypothesis, we calculated the frequency of circular RNAs overlapping with AS events and did not observe any enrichment (**Fig. 5D**), which suggested that circular RNAs were not a by-product of splicing. Furthermore, it suggests that circular RNAs may participate in the development of bamboo shoots by regulating these hub genes. Gene ontology (GO) enrichment analysis of the above described 84 hub genes giving rise to circular RNAs revealed significant enrichment mainly in cellular amino acid metabolism ($P = 7.70E-03$) and gene silencing ($P = 2.52E-02$; **Fig. 5E**), which included DEFECTIVE IN RNA-DIRECTED DNA METHYLATION 1 (*DRD1*), MAINTENANCE OF METHYLATION (*MOM*), dicer-like 3 (*DCL3*) and ARGONAUTE 1 (*AGO1*).

Interestingly, many genes associated with hub genes also produced circular RNAs. For example, the hub gene of transcription factor *bHLH93* (PH01000724G0700) which plays a role in the differentiation of stomatal guard cells (Ohashi-Ito and Bergmann 2006) produced circular exonic RNAs. Ten associated hub genes also generated circular RNAs (**Fig. 5F**). Different circular RNAs from a single cluster may coordinately modulate developmental responses of bamboo shoots. To further analyze whether the expression of circRNA species modulate transcription of their cognate linear RNA species for the hub genes in moso bamboo, we used the two-promoter vector

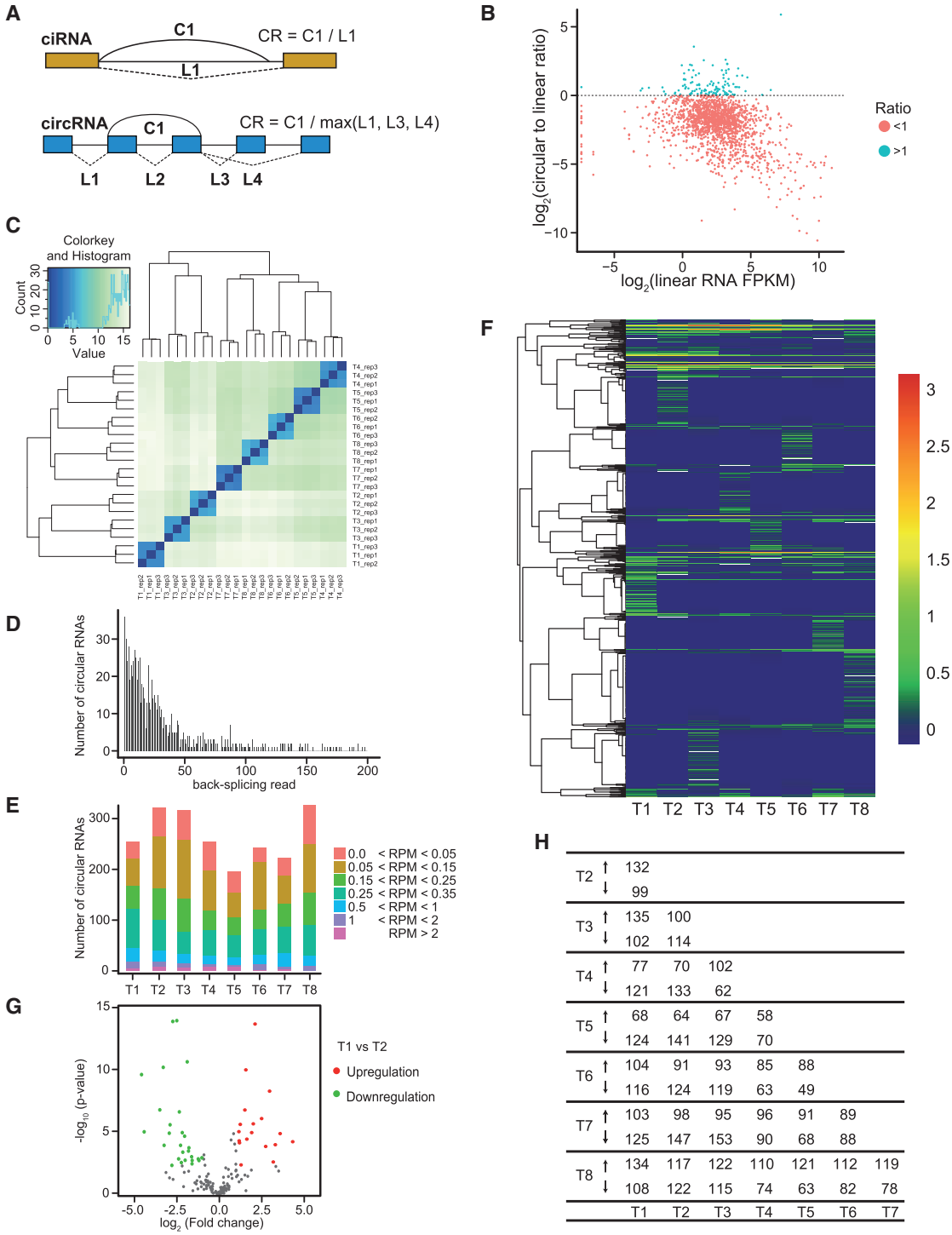

Fig. 3 Expression patterns of circular RNAs. (A) Schematic representation of the method used to calculate ratios of back-spliced junction read for circular RNAs and flanking splice junction reads for their linear counterparts. (B) Circular to linear ratio plotted against their cognate linear RNAs Fragments Per Kilobase per Million mapped reads (FPKM) shows a negative correlation between circular and their cognate linear RNAs and their numerous individual cases in which circular RNAs have higher expression levels than linear RNAs. Circular RNAs plotted in green indicated higher expression levels than linear RNAs, while red ones indicated lower expression levels than linear RNAs. (C) Hierarchical cluster analysis of circular RNAs showing that three biological replicates had a good overall correlation. (D) The number of circular RNAs and back-spliced reads identified in moso bamboo. (E) Distribution of circular RNAs abundance. The *x*-axis of the histogram presents eight different samples, which were defined as T1 (0.2 m), T2 (0.5 m), T3 (1 m), T4 (2 m), T5 (3 m), T6 (5 m), T7 (6 m) and T8 (7 m), respectively. (F) Heatmap shows the expression of circular RNA during eight shoot developmental stages. (G) Volcano plot of differentially expressed circular RNAs between T1 and T2. Red and green points represents upregulated and downregulated circular RNAs, gay points represents circular RNAs which did not expressed differently between T1 and T2. (H) The number of differentially expressed circular RNAs using pair-wise comparison. The arrows indicate upregulation and downregulation relative to the samples indicated in the bottom row.

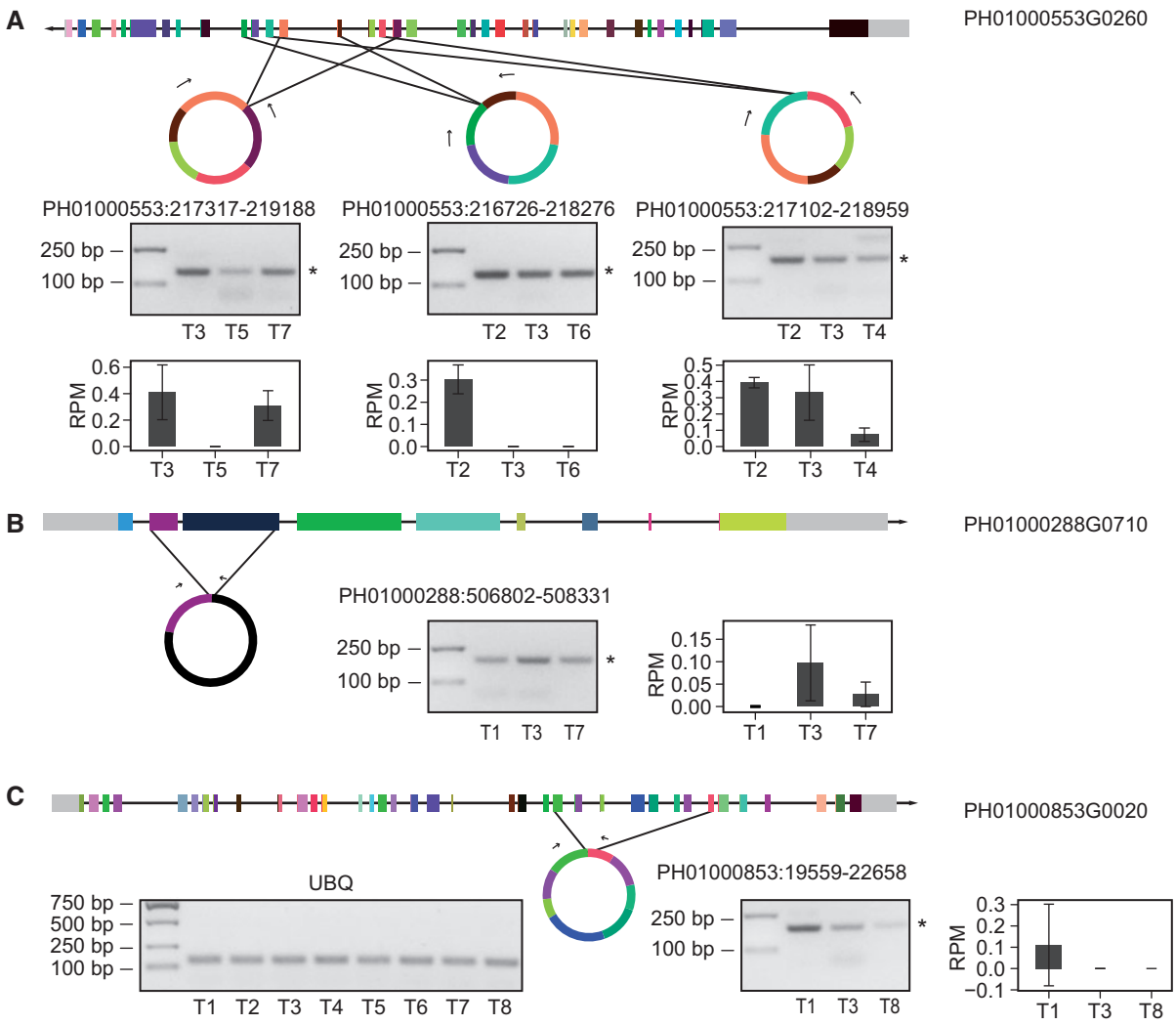

Fig. 4 RT-PCR validation of the selected circular RNAs using divergent primers. The top panel of each subfigure shows the schematics of gene structures for circular RNAs. (A) Represented three differential circular RNAs from PH01000553G0260. (B, C) Presented two circular RNAs from PH01000288G0710 and PH01000853G0020, respectively. Expected DNA fragments of five RNase R-resistant circular RNAs were amplified by RT-PCR using divergent primers. Expected PCR products from the circular RNAs junction sequences were indicated by green asterisk. Ubiquitin (UBQ) was used as internal reference. The arrows represent divergent primers. Bar plots show that the expression of circular RNAs calculated by sequence data.

system derived from pUC22-35s-sGFP (Lin et al. 2014), which included 35S promoter-driven GFP (Green Fluorescent Protein) expression to determine the transfer efficiency in protoplasts (**Fig. 5G**). Thus, the linear transcript of *bHLH93* displayed higher expression levels because the empty vector also overexpressed GFP, which might lead to higher expression level of *bHLH93*. The overexpression of *circ-bHLH93* in the other independent promoter negatively regulates the linear transcript levels of *bHLH93* (**Fig. 5H**), which suggested that *circ-bHLH93* caused the downregulated of *linear-bHLH93*. At the same time negative correlation from high-throughput sequencing has also been observed, which further supported this result. *Circ-bHLH93* and *linear-bHLH9* showed converse expression regulation during T1-T8 stages, suggested *circ-bHLH93* decreased the linear transcript during growing shoots. Together, the results revealed that *circ-bHLH93* regulates the expression of the linear transcript of its host genes according to experimental observation.

We next hypothesized that the double-stranded RNA formation between the *circ-bHLH93* and the *bHLH93* mRNA might lead to decrease of the linear RNA by generating endogenous siRNAs. To examine this hypothesis, we calculated the densities of endogenous small RNA loci in the region of *circ-bHLH93* and *bHLH93* mRNA represented by No/Lo and Ng/Lg. No and Ng represented the number of unique siRNAs mapping to the region of *circ-bHLH93* and *bHLH93* mRNA, respectively. Lo and Lg represented the length of the region of *circ-bHLH93* and *bHLH93* mRNA, respectively. We observed that the density of siRNAs in the region of *circ-bHLH93* was similar to the region of *bHLH93* mRNA (No/Lo = 0.09, Ng/Lg = 0.06, $P = 0.04$), which suggested that the endogenous siRNAs were not enriched in the region of *circ-bHLH93*. Taken together, our results revealed

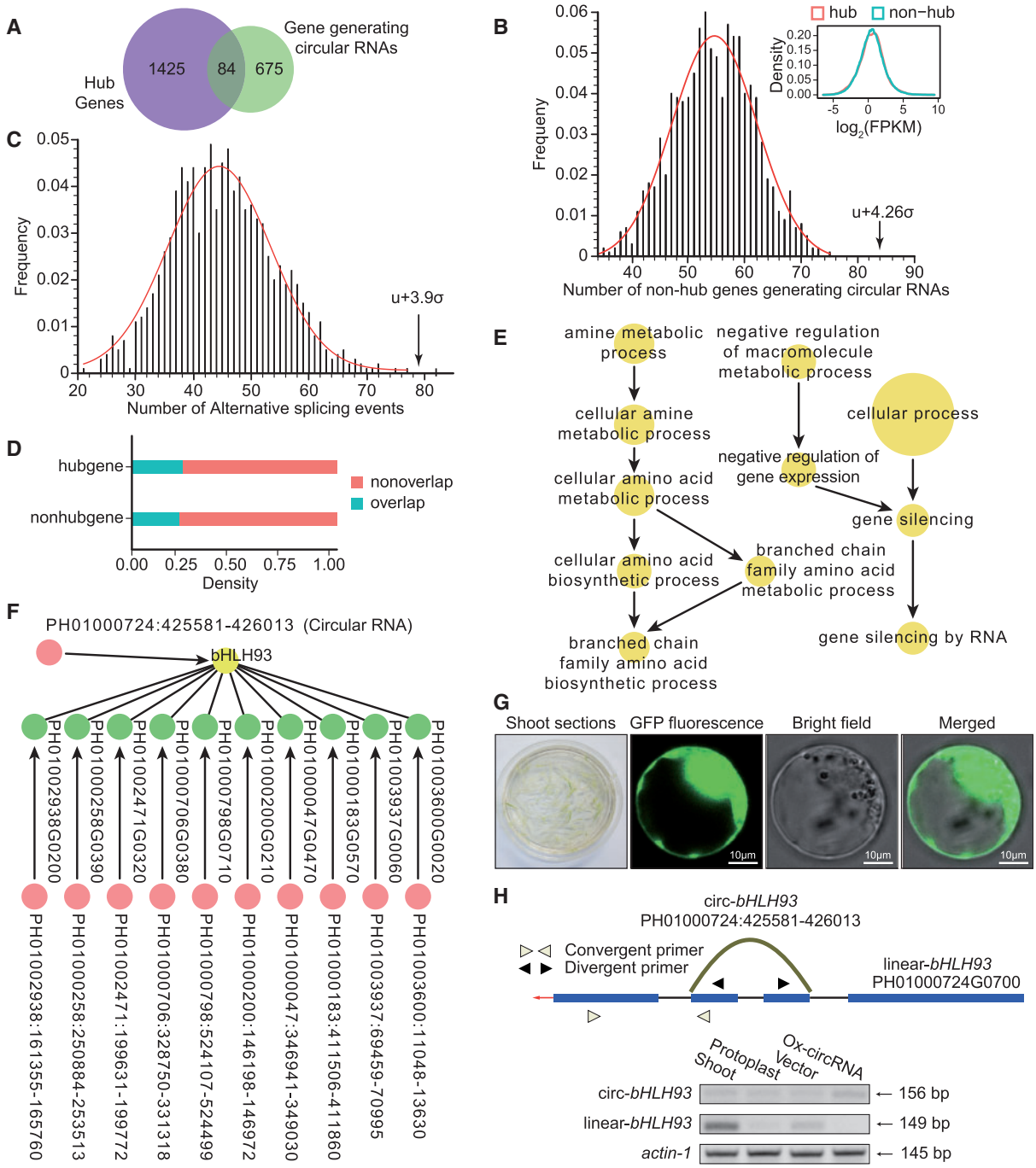

Fig. 5 Circular RNAs generated from the hub gene. (A) Venn diagrams presenting the overlap between hub genes and circular RNAs. (B) Frequency of nonhub genes generating circular RNAs. Density plot (upper right) shows that randomly selected 1,509 nonhub genes (green) with 1,000 times have similar expression level with hub genes (red). The arrow indicates the observed number of hub genes generating circular RNAs. u or σ, mean value or standard deviation of 53.5 and 4.26, respectively. (C) Frequency distribution of AS events from randomly selected genes without generating circular RNAs. The *x*-axis shows the number of AS events located in randomly selected genes without resulting circular RNAs being generated. The *y*-axis shows the frequency of the number of AS events. The solid red line is the best fit normal distribution curve. The black arrow indicates the observed number of AS events located in hub genes giving rise to circular RNAs, which is greater than the simulated mean by 3.9 times the standard deviation ($P < 0.001$). (D) The origin of AS in hub gene and nonhub gene with generating circular RNAs shows that the frequency of circular RNAs overlapped with AS events (green) is lower than that of circular RNAs outside AS events (red). (E) GO enrichment analysis for hub genes generating circular RNAs. (F) Visualization of hub-gene network between *bHLH93* (yellow) and highly connected genes. Circular RNA and 10 connected hub genes were highlighted in pink and green, respectively. Arrows indicate potential regulation of host genes. (G) Protoplast was prepared from young shoot sections of moso bamboo (left). GFP fluorescence of the control construct was checked using a confocal laser-scanning microscope indicating a successful transformation of the *circ-bHLH93* containing plasmid. (H) Schematic representation of the *circ-bHLH93* parent gene locus. The positions of divergent and convergent primer are marked with a black or white arrow head, respectively (top). Overexpression of *circ-bHLH93* negatively regulates the *linear-bHLH93* transcript in protoplast (bottom).

that the formation of double-stranded RNA between the linear circRNA precursor could not explain the downregulating of linear transcripts.

Co-expression network analysis reveals stage-specific transcription profiles

To understand the co-expression relationships among eight different developmental stages of bamboo shoots, we used differentially expressed genes for weighted gene co-expression network analysis. We identified eight developmental stage-specific co-expression modules (**Fig. 6A**), which contained 88, 30, 68, 58, 80, 58, 127 and 166 genes, respectively (**Fig. 6B** and Supplementary Table S4). Among them were 35 genes with various functions giving rise to circular RNAs. For example, *WRKY40* (PH01000043G1290) produced circular RNAs. Cellulose synthase (*CesA*), cellulose synthase–like (*Csl*) and lignin-related genes affect the formation of the cell-wall structure, which take part in the fast growth of bamboo (Peng et al. 2013a, Li et al. 2016a, Li et al. 2018). In total, 18 genes were related to rapid growth, including the cellulase A catalytic subunit gene (PH01000746G0570) that produced circular RNAs (Supplementary Table S4).

To identify dominant biological trends, we adopted GO enrichment analysis of the eight representative modules. The top 10 representative GO categories for each stage are shown in **Fig. 7A**. For example, stage-specific co-expression modules were involved in nucleotide transport (T1), regulation of dephosphorylation (T2), energy coupled proton transport (T3), auxin-mediated signaling pathway (T4), cell-wall biogenesis (T5), metabolic or biosynthetic process (T6), S-Adenosyl methionine process (T7) and protein modification (T8). Enrichment analysis revealed that specific modules represented coexpression networks in each stage with well-defined function. Circular RNAs were present in the first 10 biological processes of each modules except the T1-specific module (**Fig. 7A**). For example, *CESA1*, *UfaA1* and *TBL38* were three genes giving rise to circular RNAs, which are involved in the cell-wall organization or biogenesis in the T4- and T5-specific module (Supplementary Table S4). Interestingly, GO enrichment analysis showed that auxin-related terms were enriched in the T4-specific module (**Fig. 7B**), which included *SAUR* genes, an IAA transcriptional activator and two auxin efflux carriers (**Fig. 7C**). Three genes (PH01006019G0010, PH01000497G0760, PH01000152G0230) coexpressed with auxin-related genes also gave rise to circular RNAs (**Fig. 7B, C**), indicating that circular RNAs may affect the auxin signaling regulatory network during the rapid growth of moso bamboo shoots.

Transcriptional and post-transcriptional profiling of circular RNAs and their hosting genes

In total, we identified 759 expressed parent genes of circular RNAs throughout all eight developmental stages. Those genes were enriched in a variety of biological functions including 'structural molecules', 'transcript regulators', 'translation regulators', 'rhythmic processes' and 'developmental process' (**Fig. 8A**). Several meristem development-related terms were particularly overrepresented (**Fig. 8B**). Those categories included for instance, TOPLESS (TPL), TPL-RELATED PROTEIN (TPR)1 (TPR1) and TPR2 which are all transcriptional corepressors involved in the regulation of meristem fates in plants.

To focus on developmentally dependent changes in transcriptional expression of circular RNA and mRNA, we first hierarchically clustered mRNA transcript levels of all host genes (**Fig. 8C**). A closer inspection of the expression pattern revealed four distinct expression patterns. The majority of host genes was upregulated in the developmentally younger stages (**Fig. 8C**, orange cluster) and enriched in genes involved in 'chromatin modification', 'cell division' and 'cell cycle process' as well as in 'primary shoot apical meristem specification' (Supplementary Table S5). Expression of a small group of genes (**Fig. 8C**, green cluster) peaked at the intermediate stages and contained several genes related to 'cellulose related process' and 'glucan biosynthetic process' (Supplementary Table S5). Genes that form the yellow cluster (**Fig. 8C**) were upregulated at later developmental stages. Consistently with this expression pattern, this group was enriched in various vesical, cell membrane and cell-wall-related GO categories (Supplementary Table S5). The fourth major cluster (**Fig. 8C**, red cluster) comprised genes of various functions, which were transiently downregulated. All clusters contained a comparable number of genes giving rise to ciRNAs or circRNAs.

To determine if abundance of mRNA transcripts were related to their cognate circular RNAs on a genome-wide level, we compared the ratios of back-spliced junction reads for circular RNAs and flanking splice junction reads for their linear counterparts (**Fig. 3G**). Throughout the growth stages were different, the ratios remained fairly stable (**Fig. 8D**). The abundance of circular RNAs was with about 30% on average lower than that of their cognate linear transcripts (**Fig. 8D, E**) as reported previously (Salzman et al. 2012, Salzman et al. 2013). Notably, we also found several circular RNAs with higher abundances than the cognate mRNAs (**Fig. 8D, 8E**).

One of the essential roles of circular RNAs is to regulate the expression of their linear genes (Zhang et al. 2013, Legnini et al. 2017). To address the question of whether circular RNAs regulate parent genes in moso bamboo on a genome-wide level, we calculated the correlation between circular RNAs and parent genes. Correlation analysis showed that 287 circular RNAs 90 (76 ciRNAs and 211 circRNAs) negatively regulated their cognate linear mRNA expression, which suggested a general phenomenon that circular RNAs could decrease the levels of linear mRNA of their host genes (**Fig. 8F**). In contrast, 605 circular RNAs (98 ciRNA and 507 circRNAs) showed a moderately positive correlation (**Fig. 8F**), suggesting that parts of circRNA population promote the transcription of linear parent genes. These results suggested that the regulatory function of ciRNAs and circRNAs to the corresponding parental transcripts was diverse.

It has been recently proposed that *circ-SEP3* can result in exon skipping of its linear counterpart by forming a RNA:DNA hybrid (Conn et al. 2017). To comprehensively analyze whether AS can be regulated by circular RNA generated from their host gene, we identified AS events in T1–T8 development stages and counted the number of AS events located in the host gene that gave rise to circular RNAs. In total, 223 alternative acceptor site (AltA), 104 alternative donor sites (AltD), 78 exon skipping

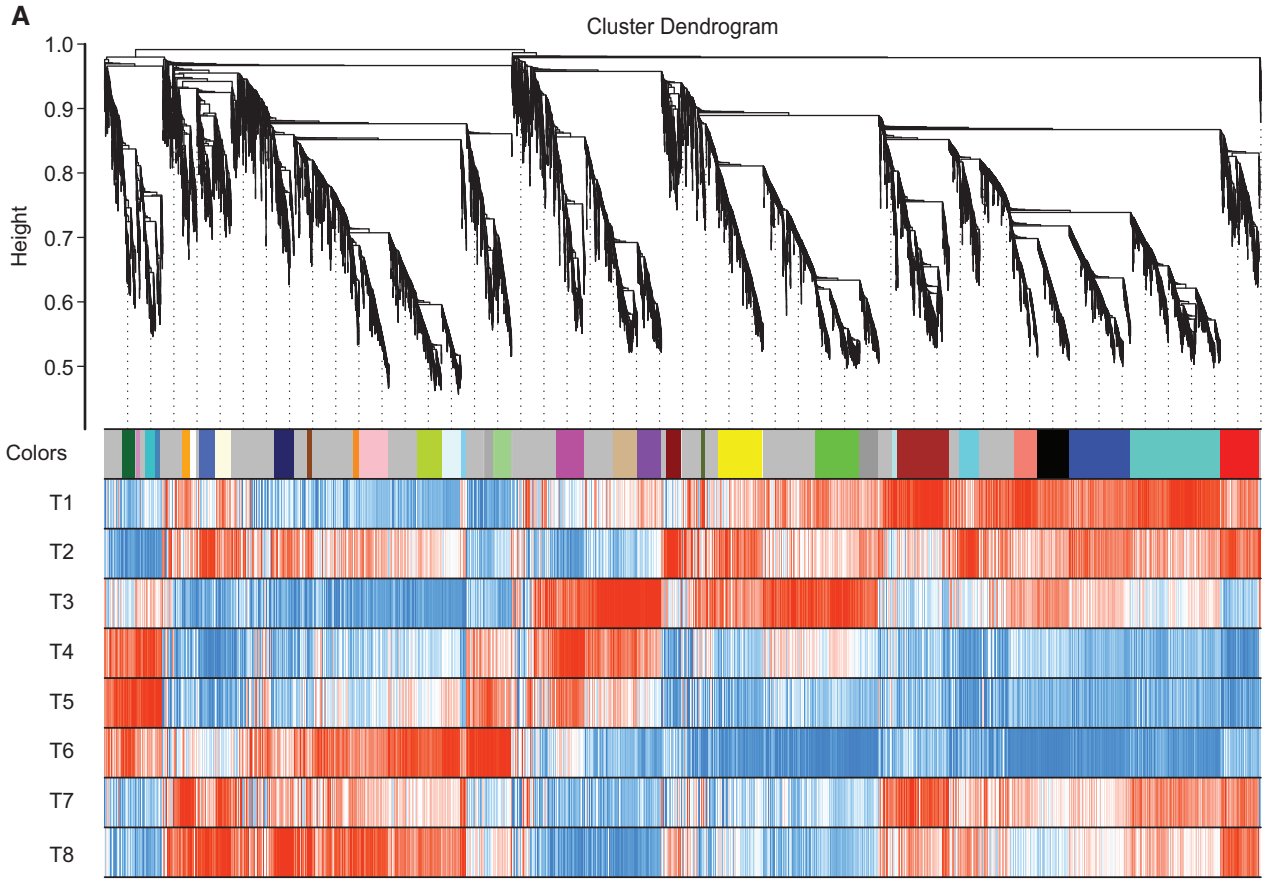

B

Modules	Gene Number	Transcription Factor	Circular RNA	Rapid growth
T1-specific Kolivegreen	88	8	4	1
T2-specific MEdarkred	30	0	2	0
T3-specific MEpurple	68	0	3	1
T4-specific MEmagenta	58	0	3	3
T5-specific MEdarkgreen	80	2	3	4
T6-specific MEdarkgrey	58	2	4	3
T7-specific darkorange	127	4	9	3
T8-specific midnightblue	166	6	7	3

Fig. 6 Coexpression modules and genes including transcription factors, circular RNAs and rapid growth-related genes. (A) WGCNA dendrogram and module colors showing coexpression modules. The first color band underneath the tree presents the modules corresponding to the hierarchical cluster tree, which were labeled with corresponding colors. The other color bands (T1–T8) represent the correlation of the different shoot developmental stages. Red represents a highly positive correlation, and blue represents negative correlation. (B) The number of transcription factors, circular RNAs and rapid growth-related genes from eight modules.

(ExonS) and 276 intron retention (IntronR) were found to be located in the host gene generating circular RNAs (**Fig. 8G** and Supplementary Table S6). To test if AS events were more significantly more enriched in genes which generated circular RNAs, we first randomly selected 759 genes without detected circular RNAs and calculated the number of four types of AS events originating from random genes. After resampling 1,000 times, the obtained simulated frequencies of AS events had significantly lower means compared with the observed number in host genes (**Fig. 8G**), which suggested that AS events were more enriched in gene that generated circular RNAs. Additionally, the Pearson correlation coefficient (r) was calculated between the circular RNA and the AS events located in their host gene, we observed that half of the number of

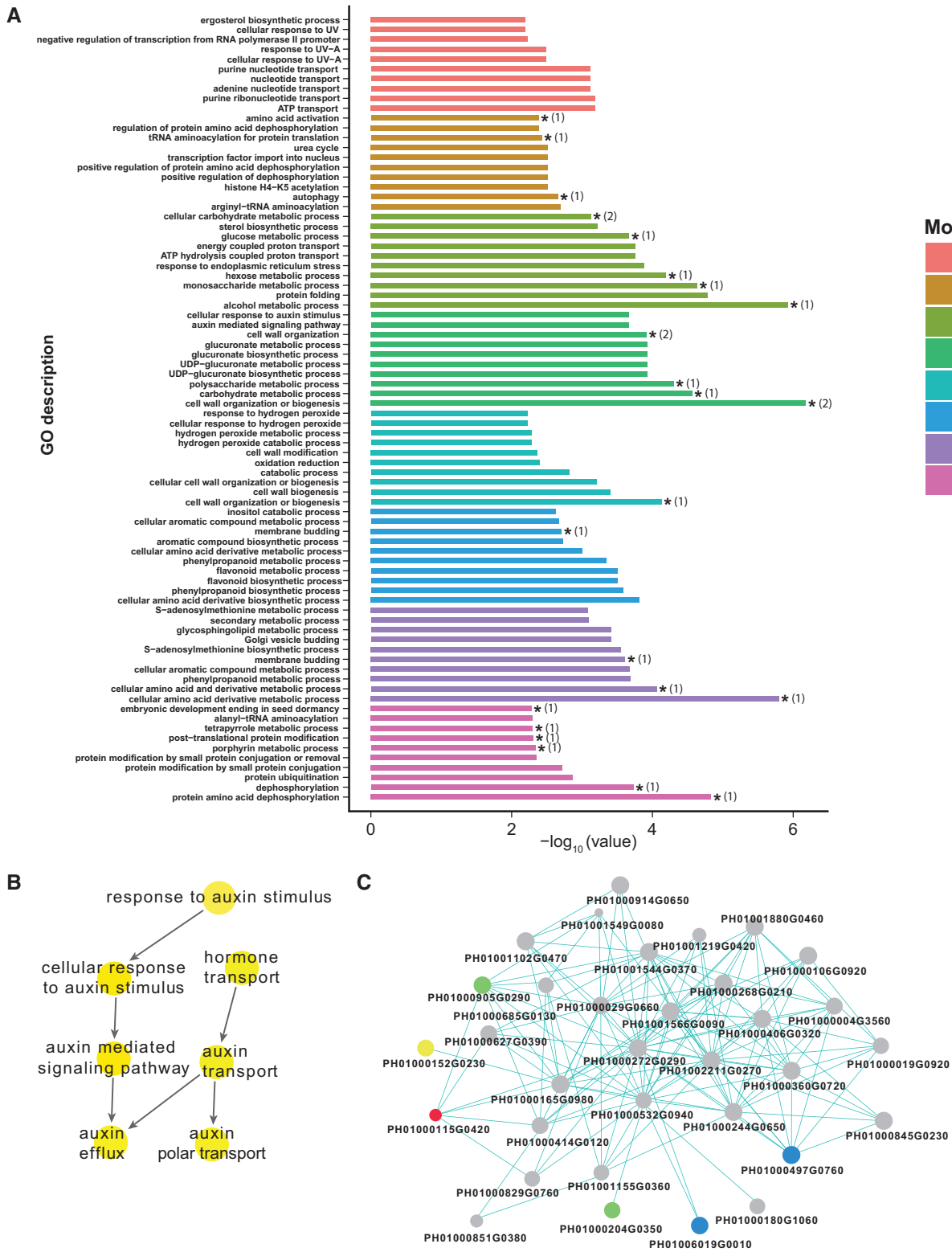

Fig. 7 Functional analysis for eight modules. (A) GO enrichment analysis for eight modules. The top representative GO terms are shown with names and *P*-values. Modules with circular RNAs are marked with an asterisk (*). The number of circRNAs are labeled corresponding to each process are given in brackets. (B) Significantly enriched GO terms related to auxin signaling and transport generating six circular RNAs in the T4-specific module, which has been labeled by MEmagenta in **Figure 6** to present highly interconnected genes associated with the T4 developmental stages. (C) Hub gene network of the highly connected genes from the T4 module. The node size indicates the number of coexpressed genes. Green nodes represented genes involved in auxin transport. Red node indicated transcription factor. Yellow node represented genes producing circular RNAs. Blue nodes indicated genes involved in rapid growth and producing circular RNAs. The gray nodes shown indicate other genes, which did not belong to TF, circular RNA and rapid growth-related genes.

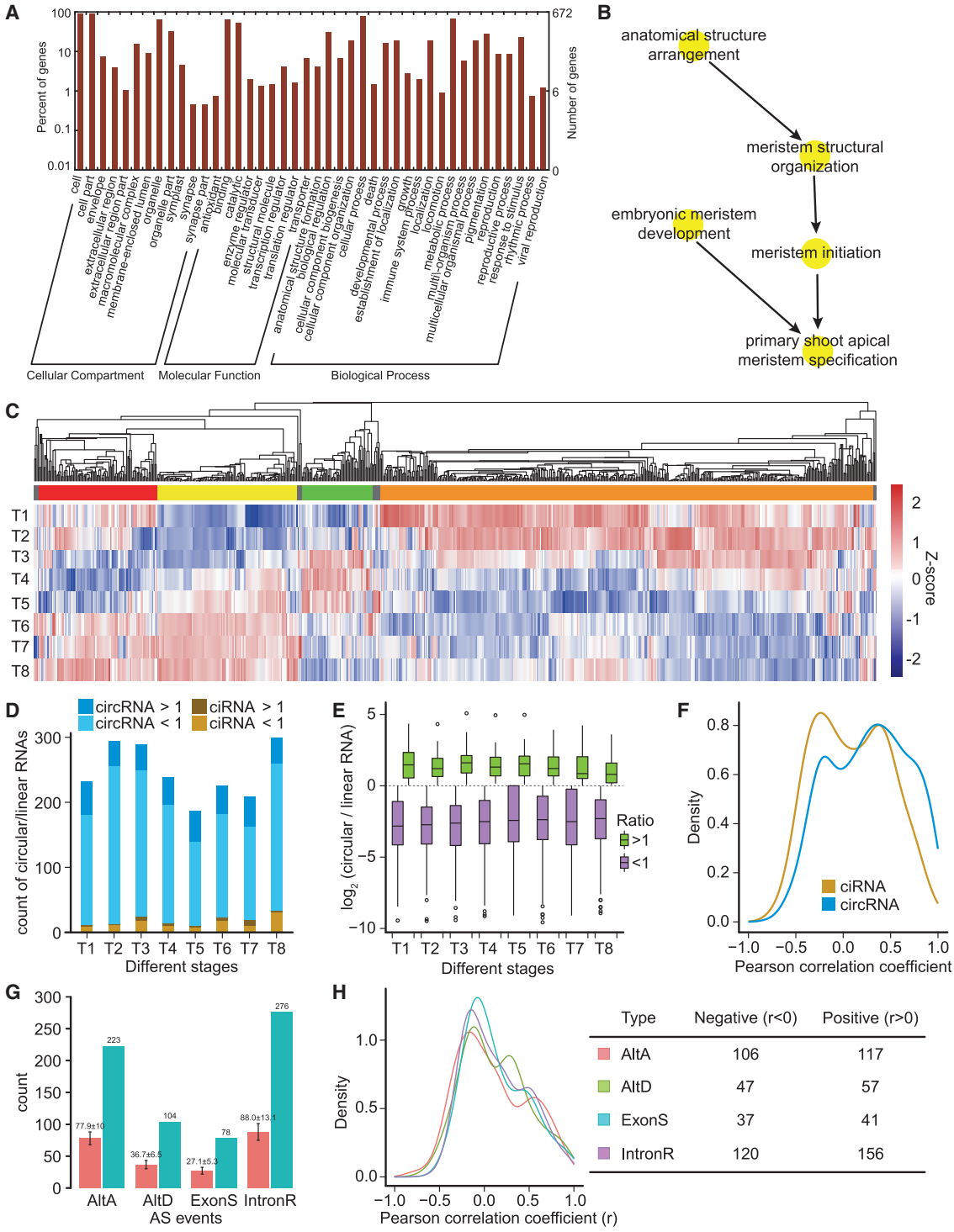

Fig. 8 Transcriptional expression of host genes in the context of circular RNAs. (A) Distribution of GO terms including percentages (left *y*-axis) and number (right *y*-axis) of host genes per GO terms. The *P*-value of the gene set enrichment is 0.05. (B) Meristem development is the main over-represented GO term for the parent genes. (C) Heatmap representing the expression patterns of parent genes. Four major clusters were defined as indicated in the color bar below the dendrogram. (D) Stacked bar chart showing the number of circular/linear RNA ratios of different categories. (E) Box plot comparing the distribution of higher (>1) or lower (<1) expressed circular RNAs compared with their cognate linear RNAs. (F) Pearson correlation coefficient (*r*) between 895 circular RNAs and 759 cognate mRNAs. The 507 circRNA and 98 ciRNA or 211 circRNA and 76 ciRNA exhibit a positive correlation ($r > 0$) or negative correlation ($r < 0$), respectively. (G) AS events enriched in the host gene gave rise to circular RNAs. Green bar indicates that the observed number of AS events located in the host gene generating circular RNAs. Red bar shows that the average number of AS located in randomly selected gene. (H) Density plot presented Pearson correlation coefficient (*r*) between the junction reads from circular RNAs and reads falling on the inclusive splicing isoform. The red, green, blue and purple lines represented the correlation between circular RNAs and four AS events (AltA, AltD, ExonS and IntronR), respectively. Table in right listed the exact numbers of circular RNAs, which presented the correlation between circular RNAs and four AS events.

circular RNAs showed a positive correlation ($r > 0$) with the corresponding AS events (**Fig. 8H**). For instance, *CESA5* (cellulose synthase A catalytic subunit 5) which is involved in the rapid growth of moso bamboo generated a circular RNA expression levels (PH01000040: 442256–443044) which highly positively correlated with intron retention events. Together, these results demonstrate an elevated AS event frequency in genes generating circular RNAs that correlates with the existence of circular RNAs.

Characterization of the regulatory network of miRNAs-circular-mRNAs

Recent reports show that circular RNAs are effective sponges for miRNAs to functionally inactivate target miRNAs (Hansen et al. 2011, Hansen et al. 2013). To investigate the regulation between circular RNAs and miRNAs, we constructed small RNA libraries for eight different stages of moso bamboo shoot development. The fragment length distribution of our small RNAs libraries was consistent with expectation (**Fig. 9A**). In total, 524 miRNAs were identified and included in the downstream analysis. To understand the possible roles of circular RNAs in regulating miRNAs, we predicted miRNA target sites within circular RNAs. In total, 197 and 78 known miRNAs were predicted to target 259 circRNAs and 68 ciRNAs, respectively (**Fig. 9B** and Supplementary Table S7). Computer simulations revealed a significantly higher frequency of miRNAs targeting circular RNAs than randomly selected short RNA fragments (**Fig. 9C**). To identify dominant biological trends for genes generating circular RNAs including miRNA binding sites, we adopted the GO enrichment analysis of genes containing miRNA target sites located in circular RNA sequences. The top 10 representative GO categories are shown in the Supplementary Table S7. They include genes involved in cell communication ($P = 0.000228$), nonsense-mediated decay ($P = 0.0066042$), and chromatin modification ($P = 0.0008985$). Intriguingly, several genes related to fast growth were included in the miRNAs targeting circular RNAs network, such as PH01001529G0090 (associated with hemicellulose metabolism) and PH01003669G0180 (associated with lignin metabolism). To further determine whether the transcript levels of miRNAs and circular RNAs were related, we calculated the Pearson correlation between miRNAs and circular RNAs, which showed negative correlation (**Fig. 9D**). In this study, we calculated Pearson correlation coefficient according to the predicted miRNAs target sites. In the future, degradome sequencing (Zhou et al. 2010) can be used to further narrow down miRNA target sites to get a more accurate correlation between miRNA and circular RNAs. However, miRNAs and parent RNAs showed positive correlation when the miRNAs target sites were located within the circular RNA sequences (**Fig. 9E**).

Subsequently, we constructed a comprehensive regulatory network of differentially expressed miRNAs, circular RNAs and mRNAs from 84 hub genes to generate a model of a possible regulatory network during moso bamboo shoot development (**Fig. 10A**). The network revealed that miRNAs could target multiple hub genes or circular RNAs, such as bamoo-miR159a and bamboo-miRNA396-3p. At the same time circular RNAs could also be targeted by several different miRNAs, such as two circular RNAs from PH01004819: 22971–32413 and PH01000012: 1644903–1645281 (**Fig. 10A**). These results suggested that circular RNAs could be involved in the development of moso bamboo shoots by interacting in a regulatory network with miRNAs and hub gene expression. To further determine whether the transcript levels of miRNAs and circular RNAs were related to each other, we performed transgenic analysis of the overexpression of miR156 including target site in *circ-TRF-1* (PH01000853: 19599–22658), which was resistant to RNase R digestion (**Fig. 10B**). The overexpression of miR156 significantly decreased the transcript levels of *circ-TRF-1* and linear transcript (**Fig. 10B**), which indicated that *circ-TRF-1* might be regulated by miR156 in moso bamboo.

Discussion

Here, with a combination of rRNA-depletion RNA-Seq and bioinformatics, we systematically characterized circular RNAs from eight different developmental stages of rapidly growing bamboo shoots. We identified several hundred circular RNAs, including 5′ and 3′ back-spliced circular RNA isoforms. It was possible that the actual number of circular RNAs was underestimated because part circular RNAs were low-abundance events. For linear transcripts, there are at least four AS types (Wang et al. 2017). Previous case studies exported that EIcircRNA showed exon skipping (Kristensen et al. 2018) and intron retention events (Li et al. 2015). However, the currently available methods cannot efficiently remove all linear RNAs in rRNA-depletion libraries (Kristensen et al. 2018). Thus, it is still not possible to identify alternative inclusion of exons or introns inside circular RNAs due to the mixture of substantial amounts of linear RNAs. In this study, we revealed a subclass of circRNA, termed here mutually inclusive circular RNAs, which, to our knowledge, has not been reported previously. Though the number may be underestimated, we are most likely to have included the most abundant types during moso bamboo shoot development. In the future, more circular RNAs for this type will be obtained by investigating more tissues and development stages.

In this study, we also detected 19 and 59 circular RNAs derived from lncRNA and natural antisense transcripts (NATs), respectively. For example, a circRNA (PH01001059: 168287–169679) derived from a lncRNA has a higher Pearson correlation ($r = 0.8$) with its upstream gene *GEBPL*, involved in redox signaling (ShaikhaLi et al. 2015) and a ciRNA (PH01004512: 50877–51018) originated from the gene *UAH* (PH01004512G0070), which was considered as a trans-NAT, involved in the catabolism of purine nucleotides (Werner et al. 2013). It will be interesting to investigate the function of these circRNAs generated from lncRNAs expressed in intergenic or antisense transcripts.

At present, biogenesis of circRNAs in plant is relatively unknown. It will be interesting to investigate major mechanisms facilitating circularization and biogenesis of circRNA in moso bamboo in the future. The flanking complementary sequences

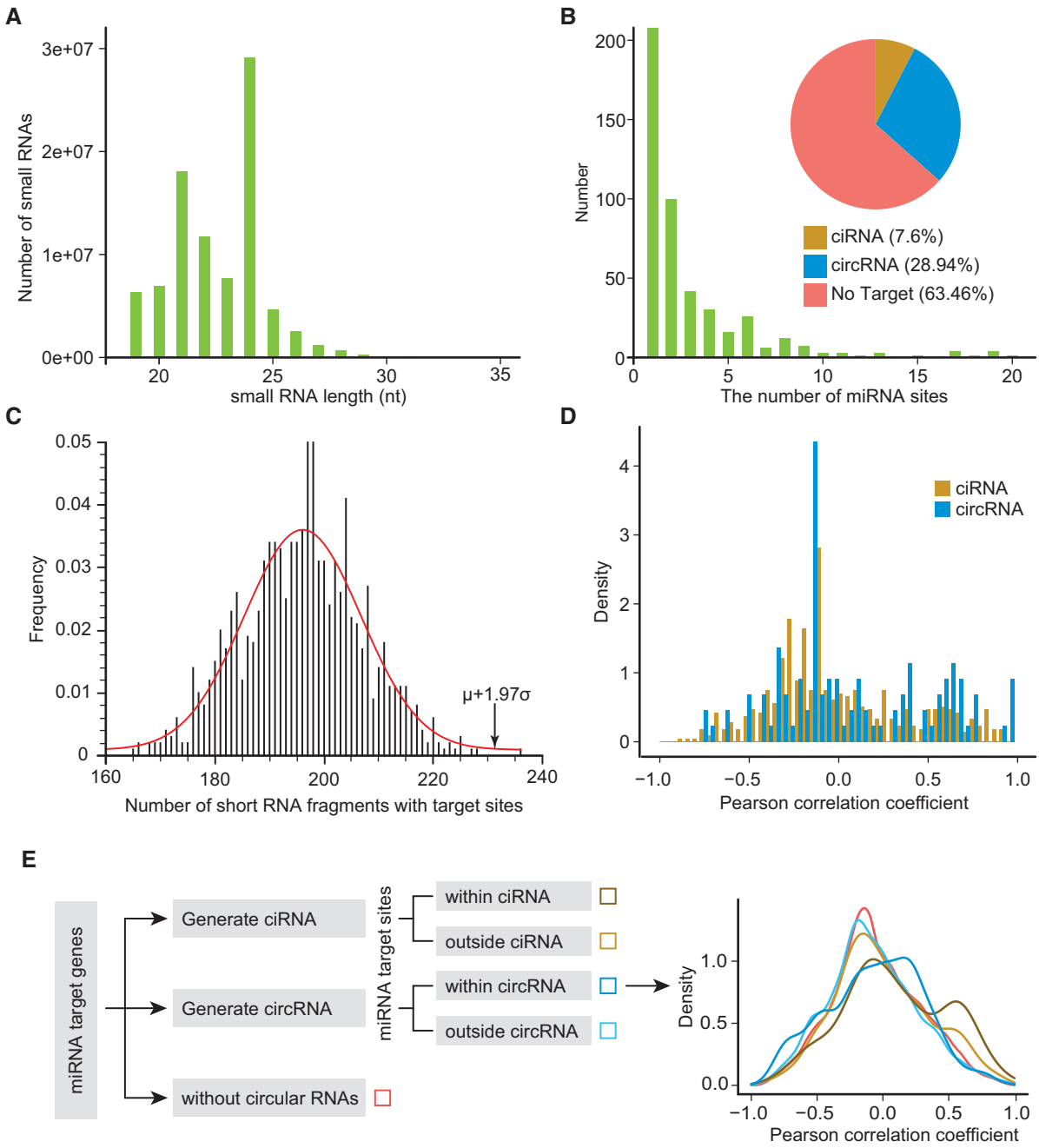

Fig. 9 miRNA target sites are enrichment in circular RNAs sequences. (A) Length distribution of the small RNA library. (B) Predicted miRNA target sites in circular RNAs. In total, 197 and 78 of 524 identified known miRNAs were predicted to target 259 circRNAs and 68 ciRNAs, respectively. (C) The frequency of miRNAs target sites increases within circular RNAs. The distribution is the frequency of randomly selected fragments contained miRNA target sties. The arrow indicates the observed number of circular RNAs targeted by miRNAs. (D) Pearson correlation coefficient (*r*) between 233 miRNAs and 327 targeted circular RNAs. Blue and yellow bars represent the correlation between miRNAs and circRNAs, miRNAs and ciRNAs, respectively. (E) Pearson correlation coefficient (*r*) between 524 miRNAs and 29,600 targeted mRNAs. Red line represents the correlation between miRNAs and its targeted mRNAs without generating circular RNAs. Deep or pale blue line represents the correlation between miRNAs and its targeted mRNAs generating circRNA which miRNAs binding sites located within or outside the sequences of circRNAs, respectively. Deep or pale yellow line represents the correlation between miRNAs and its targeted mRNAs generating ciRNA which miRNAs binding sites located within or outside the sequences of circRNAs, respectively.

were not essential for circular RNA biogenesis, as also reported by a previous study (Lu et al. 2015). However, a recent study in maize showed that LINE1-like elements are significantly enriched in the flanking regions of circRNAs (Chen et al. 2018). In our dataset, TE sequences were not enriched around flanking introns of circRNA, which suggested that TE might not play a critical role for the formation of circRNA in bamboo. The differing results may be due to the different TE percentages in the

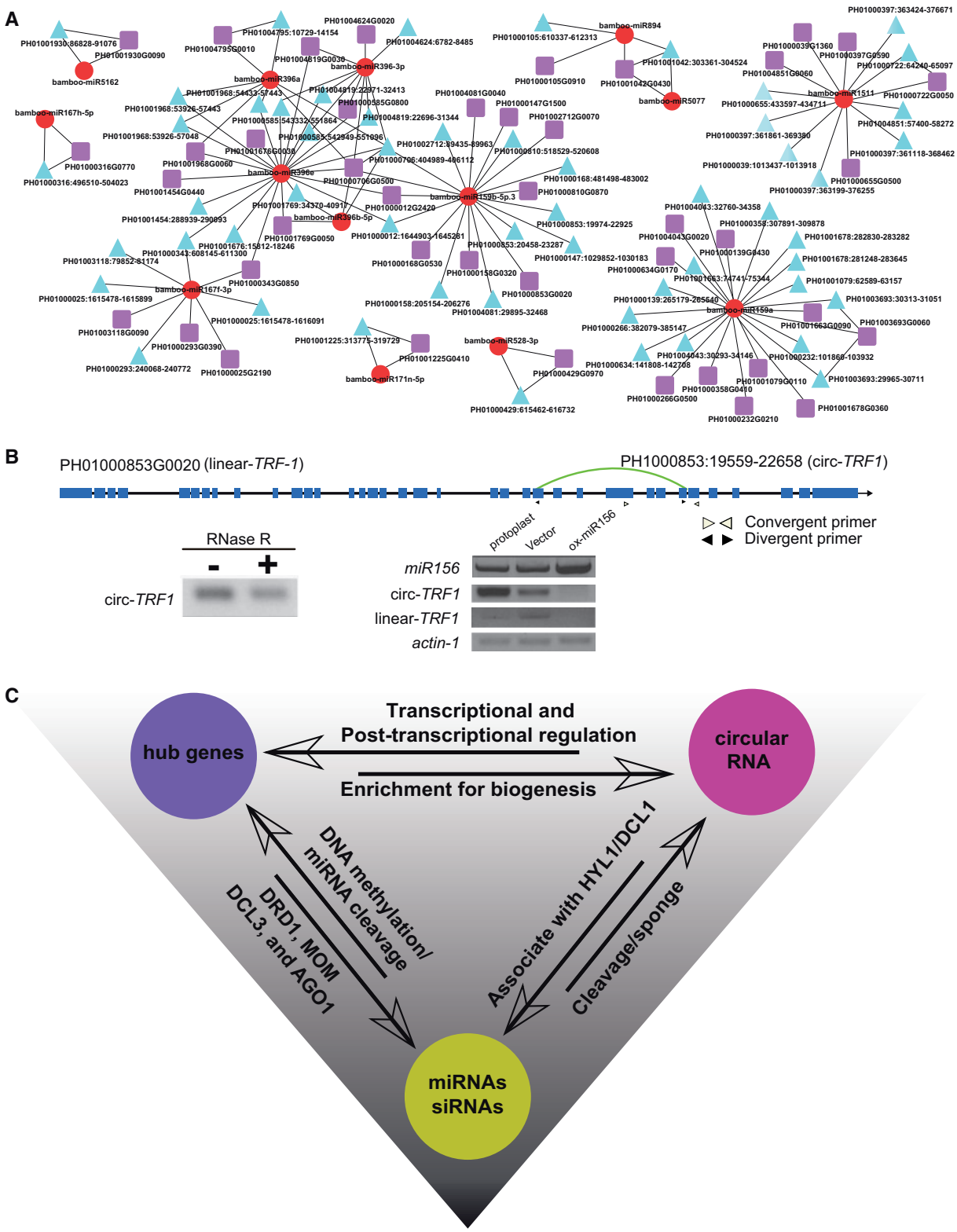

Fig. 10 Interaction among circular RNAs, miRNAs and hub genes. (A) The network of miRNAs, circular RNAs and mRNAs. Circular RNAs are represented as blue triangles, while parent genes are illustrated as purple squares. All miRNAs are displayed as red circles. (B) Schematic representation of the *circ-TRF-1* parent gene locus. The positions of divergent and convergent primer are marked with a black and white arrow head, respectively. RT-PCR validation of *circ-TRF-1* by RNase R treatment (left). Overexpression of miR156 negatively regulates the transcript levels of *circ-TRF-1* and linear-*TRF-1* in protoplast (right). (C) Hypothetical relationship of circular RNA miRNA and parent genes. Circular RNAs could be generated from several hub gene loci related to the gene silencing pathway such as, *AGO1*, *DCL3*, *DRD1* and *MOM*, which may affect the function and biogenesis of miRNA during shoot development. miRNAs target sites within circular RNAs may be a plausible regulatory mechanism for miRNAs to cleave circular RNAs. Circular RNAs may regulate parent genes at post-transcriptional levels.

two species. In maize, TE compose approximately 85% of the genome (Schnable et al. 2009). Our previous study using single-molecule long-read sequencing technology revealed many mis-annotated genes in bamboo (Wang et al. 2017). Thus, another reason for the differing results may be due to the poor annotation for intron regions surrounding flanking regions of circRNAs in bamboo. In addition, we showed that the length of exons in circRNAs originating from single exons circularization was much longer than those with multiple circularized exons (**Fig. 1E**), which might be related to a potential mechanism of circRNA biogenesis. However, the global impact of length on circRNA biogenesis has remained unclear in both mammalian and plant systems. Further experimental evidence will be required to reveal if the formation of circRNA is length-dependent. In addition to regulating canonical splicing, splicing factors may also directly affect back-splicing and circular RNA biogenesis. However, the regulation of splicing factors and their effect on the circRNA biogenesis remains unknown. In the future, it will be interesting to investigate the relationship between circRNA biogenesis and the expression of splicing factor under different temporal and spatial conditions.

Using a set of 759 corresponding host genes for GO enrichment analysis, we demonstrated their involvement in several growth-related terms such as 'cell division' and 'cell wall organization or biogenesis' (**Fig. 8A–C**). Stage-specific pattern of circular RNAs were previously reported in mammalian cells (Memczak et al. 2013). Consistent with this study, we reported differentially expressed as well as stage-specific circular RNAs in fast growing shoots of moso bamboo (**Fig. 3C**). Furthermore, several host genes were identified to be hub genes in coexpression networks demonstrating a central role of gene function for host genes and circular RNAs. Among the hub genes with generating circular RNAs, we identified several loci related to the gene silencing pathway such as *AGO1*, *DCL3*, *DRD*1 and *MOM*. In plants, primary miRNAs are trimmed to mature miRNA by DICER-LIKE1 (*DCL1*; Han et al. 2004, Yang et al. 2006, Matranga and Zamore 2007) with other cofactors, such as HYPONASTIC LEAVES1 (*HYL1*; Han et al. 2004, Vazquez et al. 2004). Mature miRNAs are subsequently loaded onto AGO1, which is involved in miRNA-mediated cleavage of target mRNAs (Baumberger and Baulcombe 2005). Recently, it has shown that circular RNAs affected the biogenesis of miRNAs by competitively inhibiting *DCL1*/*HYL1* binding with pri-miRNAs (Li et al. 2016b). Thus, the hub gene *AGO1* and circular RNAs may affect the function and biogenesis of miRNAs during shoot development, respectively (**Fig. 10C**).

In this study, gene co-expression analysis revealed two hub genes *DRD*1 and *MOM* that are well-known epigenetic regulators. *DRD1* is implicated in RNA-directed DNA methylation (RdDM) (Kanno et al. 2004) and *MOM* is essential in the transduction of RdDM signals and does not affect the levels of DNA methylation (Amedeo et al. 2000, Yokthongwattana et al. 2010). Interestingly, both *DRD1* and *MOM* gave rise to circular RNAs, which suggested that DNA methylation and circular RNAs-mediated regulatory mechanisms might not be independent processes. At present, only one study reported that genes with circular RNAs show lower DNA methylation in promoters and gene bodies (Enuka et al. 2016). However, the genome-wide impact of DNA methylation on circular RNA biogenesis is unknown in both animals and plants. It will be interesting to investigate the possible effect of DNA methylation on circular RNA biogenesis by bisulfite sequencing.

Although genome-wide profile for circular RNAs has been reported, the degradation of circular RNAs remain elusive. Circular RNAs are special because they resist breakdown through exonucleases due to their lack of the required free terminal end. Degradation mechanisms of circular RNAs are largely unknown. A previous study of animal cells revealed the function of circular RNAs as miRNAs sponges leading to the suppression of miRNA activity (Hansen et al. 2013). However, miRNA target sites within circular RNAs are also a plausible regulatory mechanism for miRNA to cleave circular RNAs in plants (**Fig. 10C**). The sequence around 10th and 11th nucleotides in miRNA may determine whether circRNAs act as sponges for miRNAs or whether the circRNAs are destined to be cleavage by miRNA. If 10th and 11th nucleotides in miRNA show a perfect match with circular RNA, miRNA may have more chances to cleavage and degrade circRNAs. Otherwise, it will be more likely that circRNAs act as miRNA sponges if the sequence pairing around the cleavage site is a mismatched loop, which is similar with target mimicry (Franco-Zorrilla et al. 2007). miRNA156 displayed high abundance in small RNA libraries and presented important function in previous reports (Wang et al. 2009, Yu et al. 2015). Thus, we selected miRNA156 as an example for protoplast transformation experiments. In this study, the overexpression of miR156 significantly decreased the transcript levels of *circ-TRF-1* (**Fig. 10B**), which indicated that *circ-TRF-1* might be cleaved by miR156 in moso bamboo. However, whether other circular RNAs cleaved by miRNA remain unknown. Thus, future experiments such as previous degradome sequencing (German et al. 2008, Zhou et al. 2010) with modifications for the identification of circular RNA degradation are needed to investigate how miRNAs and circular RNAs mechanistically interact to regulate fast growth in moso bamboo. RNA-Seq result revealed that miRNAs and target RNAs showed a positive correlation when the miRNAs target sites were located within the circular RNA sequences (**Fig. 9E**), which supports previous findings that some circular RNAs could also function as positive regulators of their linear transcripts by competing with miRNA targeted sites (Memczak et al. 2013, Lu et al. 2015). Taken together, these results suggest that circular RNAs can act as miRNA sponges and can also be degraded by miRNAs in moso bamboo.

The currently disclosed functions of circular RNAs have presented diversity status, such as miRNA sponges (Hansen et al. 2013, Huang et al. 2017), regulation of splicing (Zhang et al. 2013, Li et al. 2015) and affecting transcription of the parental gene by interaction with RNA polymerase and U1 snRNP (Li et al. 2015). According to RNA-Seq result, we calculated the Pearson correlation coefficient (r) between circular RNAs and their linear RNAs. In total, 287 circular RNAs showed the negative Pearson correlation coefficient with their cognate mRNAs, which suggested a general phenomenon that circular RNAs could decrease the levels of linear mRNA of their host genes. The overexpression of *circ-bHLH93* further validated the

negative correlation with its linear transcripts. However, we still could not exclude the possible that circular RNAs might affect the expression of many other different linear transcripts in addition to their host genes. For example, circular RNAs from transcript factors might affect the host transcripts, which might further affect many other different linear transcripts. It has been reported that circular RNAs could act in *trans* to regulate other nonparental genomic loci (Ebbesen et al. 2016). However, the impact of indirect regulation will be hard to find out downstream targets. Thus, protoplast transformation experiment in this study only focused the regulation of circular RNAs on their own host genes. Circular RNAs could decrease the levels of linear RNAs by competing with canonical splicing (Salzman et al. 2012), which were further validated by diminishing the elongation capacity of RNA polymerase II and showing negative correlation between the efficiency of canonical splicing and the level of circular RNAs biogenesis (Ashwal-Fluss et al. 2014). Moreover, circular RNA such as *CDR1as* and *CircHIPK2* can also act as miRNA sponges which might contribute to the activity of miRNAs on the expression level of target genes including the host gene (Hansen et al. 2013, Huang et al. 2017). Finally, a case study showed that *circ-SEP3* regulates exon skipping of its cognate DNA locus by forming an RNA: DNA hybrid (Conn et al. 2017). R-loop results suggested that circular RNAs could regulate the canonical splicing of linear transcripts to produce different isoforms, which might be interplay with miRNA target sites to affect the linear mRNA degradation (Wang et al. 2019). In our study, we observed that the host genes with the existence of circular RNAs had a higher frequency of AS events generation and half of the circular RNAs displayed a positive correlation with the corresponding AS events in eight different developmental stages of moso bamboo. Moreover, several circular RNAs and their highly relevant AS events originated from genes related to rapid growth, such as CESA5 (cellulose synthase A catalytic subunit 5). Our results suggest that circular RNA might play an important role in development of moso bamboo by regulating the splicing of several rapid-growth-related genes. It will be interesting to investigate whether the circular RNAs from these loci can regulate the transcription or post-transcriptional modifications of hub genes especially for miRNA-related genes such as *AGO1*, *DCL3*, *DRD1* and *MOM*. This study shows that the interactions of circRNAs, miRNAs and parent hub genes might provide a novel perspective to regulate the fast growth of moso bamboo shoots (**Fig. 10C**).

Materials and Methods

Sample collection and library construction

Bamboo shoot samples from eight different heights were collected in May of 2017 from the botanical garden of bamboo at Fujian Agriculture and Forestry University in the Fujian Province of China (E119°14′; N26°05′). Bamboo shoots were classified according to their heights above the ground as T1 (0.2 m), T2 (0.5 m), T3 (1 m), T4 (2 m), T5 (3 m), T6 (5 m), T7 (6 m) and T8 (7 m), respectively. Three independent biological replicates from T1 to T8 stages were collected, and then the middle internodes were obtained and immediately frozen in liquid nitrogen and stored at −80°C. Total RNA was extracted from these samples with the RNAprep Pure Plant Kit (Tiangen, Cat. #DP441, China).

RNA-seq library preparation and sequencing

rRNA was removed using the Ribo-Zero Magnetic kit with 5 μg RNA as input material for each library. Then, strand-specific RNA-Seq libraries were constructed by dUTP strand-specific library protocol, as described previously (Wu et al. 2014, Wang et al. 2017). In brief, DNA fragments of 400–500 bp in length were isolated from 2% agarose gel. Then dUTP strand-specific libraries were sequenced using an Illumina HiSeq 2500 platform to generate 125 nt paired-end reads.

Functional annotation of moso bamboo

In this study, GO terms were obtained using WEGO (Ye et al. 2018) and BLAST2GO (Conesa et al. 2005) with default options. Homolog genes of moso bamboo were identified in *Arabidopsis* using InParanoid (version 3.0) with default options (Ostlund et al. 2010). We then searched for splicing-related genes in moso bamboo by using the identified homologs in the *Arabidopsis* Splicing Related Genes (ASRG) database (Wang and Brendel 2004).

Identification of circular RNAs from rRNA-depleted libraries

The reads generated from the HiSeq 2500 platform were filtered using the HTQC package (v-1.92.1) with the default parameters to remove low-quality reads (Yang et al. 2013). Clean reads were aligned to the bamboo genome using Tophat (v-2.0.11) using the following option: –fusion-search –keep-fasta-order –bowtie1 –no-coverage-search -r 0 –mate-std-dev 80 –max-intron-length 100000 –fusion-min-dist 100000 –fusion-anchor-length 20 (Trapnell et al. 2009). The above un-contiguously aligned reads and the annotation of bamboo were then used as input for the CIRCexplorer program (v-1.1.10) to identify circular RNAs by the circularizing junction alignment (Zhang et al. 2014). As the annotation of moso bamboo only include the coding genes (Peng et al. 2013b), lncRNAs (Wang et al. 2017) and NATs (Zhang et al. 2018) were obtained from publicly available data. The circular RNAs were detected with at least one back-spliced junction read by CIRCexplorer according to gene annotation. Multimapped junction reads were filtered out. Mutually inclusive circular RNAs were detected by searching for events including overlapping coordinate regions with different back-splicing donor and acceptor sites. Circular RNAs in *Arabidopsis* (Li et al. 2016b) and *O. sativa* (Secco et al. 2013) were identified using publicly available high-throughput sequencing data from SRP062035, SRR1005257 and SRR1005260, respectively. Reference sequences and the annotation of *Arabidopsis* (TAIR10) and *O. sativa* (MSU6.1) were obtained from TAIR (http://www.arabidopsis.org) and the MSU Genome Annotation Project Database (http://rice.plantbiology.msu.edu), respectively.

Due to the limitation of read length, we cannot calculate the length of circular RNAs using reads from body regions of circular RNAs. Thus, the length of circular RNAs was calculated by the back-splicing junction reads, which included precise coordinate information about the start and end of circular RNAs. Expression of circular RNAs was calculated using the circular back-spliced junction read, which aligned to the same gene locus with nonlinear ordering. In this study, we used only junction reads and excluded other non-head-to-tail junction reads enclosed within circular RNAs for the quantitative comparison. Circular RNAs abundance was further normalized to RPM. The *P*-value and False Discovery Rate (FDR) was calculated using the edgeR package (Robinson et al. 2010). Differential expressed circular RNAs were identified using fold change > 2 and FDR < 0.01 as cutoff. BINGO was used for GO enrichment analysis (Maere et al. 2005).

Experimental validation of circular RNA

Divergent primers were designed to cross the back-spliced junction using PRAPI (Gao et al. 2017). A total of 20 μg RNAs were dissolved in 51 μl DEPC treated water and split into two RNase-free microcentrifuge tubes: one for RNase R digestion, and another for control. In total, 3 μl 10×RNase R Reaction Buffer and 1.5 μl RNase R (20 U/μl) were added for RNase R digestion and incubated for 15 min at 37°C. For the control sample, 3 μl 10×RNase R Reaction Buffer and 1.5 μl DEPC-treated water were added and incubated under the same conditions. After the incubation step, 30 μl of phenol–chloroform–isoamyl alcohol were added to stop the exonuclease digestion. The samples were spun in

a microcentrifuge at 13,000×*g* at 4°C for 5 min. The supernatant was transferred to a new 1.5 ml RNase-free microcentrifuge tube that contained 6 µl 4 M LiCl, 1 µl glycogen and 90 µl prechilled absolute ethanol (−20°C). Then the mixture was inverted gently and stored at -80°C for 1 h. Finally, the RNA treated with RNase R was reverse-transcribed to cDNA. For each PCR amplification, 1 µl of cDNA with 15 µl Premix Taq (Takara), 0.5 µl forward primer, 0.5 µl reverse primer and 13 µl ddH_2O were mixed, and the PCR cycle was run for 40 cycles. PCR products with predicted sizes were visualized and dissected from an agarose gel. Divergent primers for circular RNAs and regular NTB primers used for RT-PCR were listed in Supplementary Table S8.

RNAs were reverse-transcribed using the PrimeScriptTM II 1st Strand cDNA Synthesis Kit (Takara, cat.no.6210A) with 1 µg total RNA and random 6-mers (50 µM). Circular RNAs were amplified and quantified by semi-quantitative PCR using Premix TaqTM (Takara TaqTM Version 2.0 plus dye, cat.no. RR901A) with 1/10 diluted cDNA as the template. For all experiments, UBQ was used as a normalization control. PCR products with the expected sizes were visualized on a 2% agarose gel stained with GelStain (TransGen, cat.no.GS101-03). The full list for all the primers is shown in Supplementary Table S8.

Identification of differential expressed mRNAs and AS events from RNA-Seq data

Low-quality reads from eight stages were removed by the HTQC package (v-1.92.1) with the default options selected (Yang et al. 2013). The remaining reads were mapped to the Moso bamboo genome (Peng et al. 2013b) with parameters '-r 50 -a 8' using tophat (v-2.0.11; Trapnell et al. 2009). Differentially expressed genes were identified using a combination of 2-fold change which was calculated based on FPKM values and a FDR smaller than 0.01 calculated using the edgeR package (Robinson et al. 2010). Aligned reads were used to generate transcriptome assemblies applying Cufflinks (v-2.1.1) with the following option '-F 0.05 -A 0.01 -I 100000 –min-intron-length 30' (Trapnell et al. 2012). Differential AS events were identified using rMATS.3.2.2 with following option '-len 125 -a 8 -c 0.0001 -analysis U -t paired' (Shen et al. 2014). To determine whether the number of AS events located in genes producing circular RNAs was significantly higher than that of genes without circular RNAs, we randomly selected the same number of genes not generating circular RNAs and identified four types of AS. The simulation was repeated 1,000 times.

Small RNA-Seq and bioinformatics analysis

Small RNA was enriched using PEG8000 precipitation from 5 µg of total RNA for each library. The 16–44 nt small RNAs were isolated using 15% PAGE after the 3′-linker was added. The sample was then reversed transcribed after adding the 5′-linker. The final DNA product was isolated using 3.5% PAGE and bands of 160 bp size were isolated and sequenced using HiSeq 2500 according to the manufacturer's instructions.

The adapter sequences of raw reads were removed using fastx_clipper of the FASTX toolkit (http://hannonlab.cshl.edu/fastx_toolkit/) from Gregory Hannon's laboratory. Bowtie 2 (v2.2.1) was used for the alignment of small RNAs (Langmead and Salzberg 2012). miRNAs were identified using BLAST searching the current release of miRBase (v21; Kozomara and Griffiths-Jones 2013) using e-value < 0.05, less than three-mismatches and without gap alignment. The expression of miRNAs was calculated as RPM. The *P*-value and FDR was inferred using the edgeR package (Robinson et al. 2010). Differentially expressed miRNAs were identified using fold change >2 and FDR < 0.01 as the cutoff. The target sites were predicted using miRferno.py from the sPARTA package using the following option: -genomeFeature 0 -tarPred -tarScore (Kakrana et al. 2014). To determine whether miRNAs compared with other small RNAs are targeting circular RNAs to a significantly higher level, we randomly selected 542 small RNAs with 21 nt from small RNA libraries and predicted possible target sites located within circular RNAs. The simulation was repeated 1,000 times.

Co-expression networks and hub genes

The differentially expressed genes identified in this study were used to construct co-expression networks with the R package WGCNA (Langfelder and Horvath 2008). Visual analysis of the constructed networks and GO enrichment were represented using Cytoscape 3.5.1. To determine whether the number of circular RNAs from hub genes was significantly higher than that of nonhub genes, we randomly selected the same number of nonhub genes with similar expression levels to hub genes and calculated the number of genes giving rise to circular RNAs. The simulation was repeated 1,000 times.

Protoplast isolation, plasmid construction and protoplast transfection

Shoot protoplasts of moso bamboo were isolated and transformed as previously described (Zhang et al. 2011) with minor modifications. In brief, the seedlings of moso bamboo were grown on soil for 2 weeks. Then shoots of moso bamboo were cut into pieces and incubated in an enzyme solution (1.5% Cellulase RS, 0.75% Macerozyme R-10, 0.6 M mannitol, 10 mM MES at pH 5.7, 10 mM $CaCl_2$ and 0.1% BSA) for 3 h in the dark with gentle shaking (50 rpm) at 25°C. Protoplasts were filtered through a nylon mesh, washed (154 mM NaCl, 125 mM $CaCl_2$, 5 mM KCl and 2 mM MES at pH 5.7) and pelleted (1,500 rpm for 3 min). After additional washing steps, protoplasts were resuspended in MMG solution (0.4 M mannitol, 15 mM $MgCl_2$ and 4 mM MES at pH 5.7).

In this study, we used the two-promoter vector system derived from pUC22-35s-sGFP, which carried 35S promoter-driven GFP expression to confirm successful transformation into protoplasts and transfer efficiency (Lin et al. 2014). Sequences of *circ-bHLH93* (PH01000724: 425581–426013) including the endogenous flanking sequences were cloned into an independent promoter to overexpress the circRNA species of *bHLH93*. Divergent and convergent primers were used to detect the circRNA and the linear RNA from the host gene, respectively, by semi-quantitative RT-PCR. Primer sequences are listed in Supplementary Table S8. The protoplasts were observed with a confocal laser-scanning microscope (Leica TCS 5 SP5 X) and visualized by a Leica Microsystem LAS X 3.1.1.

Supplementary Data

Supplementary data are available at PCP online.

Funding

This work was supported by the National Key R&D Program of China [2018YFD0600101 and 2016YFD0600106], the National Natural Science Foundation of China Grant [31570674 and 31800566], the International Science and Technology Cooperation and Exchange Fund from Fujian Agriculture and Forestry University [KXGH17016], Natural Science Foundation of Fujian Province of China [Grant No. 2018J01608] and Program for scientific and technological innovation team in university of Fujian province [No. 118/KLA18069A] to generate the data.

Author Contributions

C.L. and L.G. conceived the study. Y.W., H.W., X.L., X.X., K.H., and L.Z. performed the experiments. Y.W., Y.G., H.Z., Z.Z., M.V.K., H.W. and F.X. analyzed the high-throughput sequencing data. L.G. supervised the project and wrote the manuscript. All authors have read and approved the final version.

Disclosures

The authors have no conflicts of interest to declare.

References

Amedeo, P., Habu, Y., Afsar, K., Scheid, O.M. and Paszkowski, J. (2000) Disruption of the plant gene MOM releases transcriptional silencing of methylated genes. *Nature* 405: 203.

Ashwal-Fluss, R., Meyer, M., Pamudurti, N.R., Ivanov, A., Bartok, O. and Hanan, M. (2014) circRNA biogenesis competes with pre-mRNA splicing. *Mol. Cell.* 56: 55–66.

Baumberger, N. and Baulcombe, D. (2005) Arabidopsis ARGONAUTE1 is an RNA Slicer that selectively recruits microRNAs and short interfering RNAs. *Proc. Natl. Acad. Sci. USA* 102: 11928–11933.

Beermann, J., Piccoli, M.-T., Viereck, J. and Thum, T. (2016) Non-coding RNAs in development and disease: background, mechanisms, and therapeutic approaches. *Physiological reviews* 96: 1297–1325.

Burd, C.E., Jeck, W.R., Liu, Y., Sanoff, H.K., Wang, Z. and Sharpless, N.E. (2010) Expression of linear and novel circular forms of an INK4/ARF-associated non-coding RNA correlates with atherosclerosis risk. *PLoS Genet.* 6: e1001233.

Capel, B., Swain, A., Nicolis, S., Hacker, A., Walter, M., Koopman, P., et al. (1993) Circular transcripts of the testis-determining gene Sry in adult mouse testis. *Cell* 73: 1019–1030.

Chen, H.C. and Cheng, S.C. (2012) Functional roles of protein splicing factors. *Biosci. Rep.* 32: 345–359.

Chen, L., Zhang, P., Fan, Y., Lu, Q., Li, Q., Yan, J., et al. (2018) Circular RNAs mediated by transposons are associated with transcriptomic and phenotypic variation in maize. *New Phytol.* 217: 1292–1306.

Chen, L.-L. (2016) The biogenesis and emerging roles of circular RNAs. *Nat. Rev. Mol. Cell Biol.* 17: 205–211.

Conesa, A., Gotz, S., Garcia-Gomez, J.M., Terol, J., Talon, M. and Robles, M. (2005) Blast2GO: a universal tool for annotation, visualization and analysis in functional genomics research. *Bioinformatics* 21: 3674–3676.

Conn, V.M., Hugouvieux, V., Nayak, A., Conos, S.A., Capovilla, G., Cildir, G., et al. (2017) A circRNA from SEPALLATA3 regulates splicing of its cognate mRNA through R-loop formation. *Nat. Plants.* 3: 17053.

Djebali, S., Davis, C.A., Merkel, A., Dobin, A., Lassmann, T., Mortazavi, A., et al. (2012) Landscape of transcription in human cells. *Nature* 489: 101–108.

Ebbesen, K.K., Kjems, J. and Hansen, T.B. (2016) Circular RNAs: identification, biogenesis and function. *Biochim. Biophys. Acta.* 1859: 163–168.

Enuka, Y., Lauriola, M., Feldman, M.E., Sas-Chen, A., Ulitsky, I. and Yarden, Y. (2016) Circular RNAs are long-lived and display only minimal early alterations in response to a growth factor. *Nucleic Acids Res.* 44: 1370–1383.

Franco-Zorrilla, J.M., Valli, A., Todesco, M., Mateos, I., Puga, M.I., Rubio-Somoza, I., et al. (2007) Target mimicry provides a new mechanism for regulation of microRNA activity. *Nat. Genet.* 39: 1033–1037.

Gao, Y., Wang, H., Zhang, H., Wang, Y., Chen, J. and Gu, L. (2017) PRAPI: post-transcriptional regulation analysis pipeline for Iso-Seq. *Bioinformatics* 1: 3.

German, M.A., Pillay, M., Jeong, D.-H., Hetawal, A., Luo, S., Janardhanan, P., et al. (2008) Global identification of microRNA–target RNA pairs by parallel analysis of RNA ends. *Nat. Biotechnol.* 26: 941.

Guo, J.U., Agarwal, V., Guo, H.L. and Bartel, D.P. (2014) Expanded identification and characterization of mammalian circular RNAs. *Genome Biol*. 15: 409.

Han, M.H., Goud, S., Song, L. and Fedoroff, N. (2004) The Arabidopsis double-stranded RNA-binding protein HYL1 plays a role in microRNA-mediated gene regulation. *Proc. Natl. Acad. Sci. USA* 101: 1093–1098.

Hansen, T.B., Jensen, T.I., Clausen, B.H., Bramsen, J.B., Finsen, B., Damgaard, C.K., et al. (2013) Natural RNA circles function as efficient microRNA sponges. *Nature* 495: 384–388.

Hansen, T.B., Wiklund, E.D., Bramsen, J.B., Villadsen, S.B., Statham, A.L., Clark, S.J., et al. (2011) miRNA-dependent gene silencing involving Ago2-mediated cleavage of a circular antisense RNA. *EMBO J.* 30: 4414–4422.

Hsu, M.-T. and Coca-Prados, M. (1979) Electron microscopic evidence for the circular form of RNA in the cytoplasm of eukaryotic cells. *Nature* 280: 339–340.

Huang, R.R., Zhang, Y., Han, B., Bai, Y., Zhou, R.B., Gan, G.M., et al. (2017) Circular RNA HIPK2 regulates astrocyte activation via cooperation of autophagy and ER stress by targeting MIR124-2HG. *Autophagy* 13: 1722–1741.

Jeck, W.R. and Sharpless, N.E. (2014) Detecting and characterizing circular RNAs. *Nat. Biotechnol.* 32: 453–461.

Jeck, W.R., Sorrentino, J.A., Wang, K., Slevin, M.K., Burd, C.E., Liu, J., et al. (2013) Circular RNAs are abundant, conserved, and associated with ALU repeats. *RNA* 19: 141–157.

Kakrana, A., Hammond, R., Patel, P., Nakano, M. and Meyers, B.C. (2014) sPARTA: a parallelized pipeline for integrated analysis of plant miRNA and cleaved mRNA data sets, including new miRNA target-identification software. *Nucleic Acids Res*. 42: e139.

Kanno, T., Mette, M.F., Kreil, D.P., Aufsatz, W., Matzke, M. and Matzke, A.J. (2004) Involvement of putative SNF2 chromatin remodeling protein DRD1 in RNA-directed DNA methylation. *Curr. Biol.* 14: 801–805.

Kozomara, A. and Griffiths-Jones, S. (2014) miRBase: annotating high confidence microRNAs using deep sequencing data. *Nucleic Acids Res.* 42: D68–D73.

Kristensen, L., Hansen, T., Venø, M. and Kjems, J. (2018) Circular RNAs in cancer: opportunities and challenges in the field. *Oncogene* 37: 555–565.

Langfelder, P. and Horvath, S. (2008) WGCNA: an R package for weighted correlation network analysis. *BMC Bioinformatics* 9: 559.

Langmead, B. and Salzberg, S.L. (2012) Fast gapped-read alignment with Bowtie 2. *Nat. Methods.* 9: 357–359.

Legnini, I., Di Timoteo, G., Rossi, F., Morlando, M., Briganti, F., Sthandier, O., et al. (2017) Circ-ZNF609 is a circular RNA that can be translated and functions in myogenesis. *Mol. Cell.* 66: 22–37.e9.

Li, L., Cheng, Z., Ma, Y., Bai, Q., Li, X., Cao, Z., et al. (2018) The association of hormone signaling genes, transcription, and changes in shoot anatomy during moso bamboo growth. *Plant Biotechnol. J.* 16: 72–85.

Li, L., Hu, T., Li, X., Mu, S., Cheng, Z., Ge, W., et al. (2016a) Genome-wide analysis of shoot growth-associated alternative splicing in moso bamboo. *Mol. Genet. Genomics* 291: 1695–1714.

Li, Z., Huang, C., Bao, C., Chen, L., Lin, M., Wang, X., et al. (2015) Exon-intron circular RNAs regulate transcription in the nucleus. *Nat. Struct. Mol. Biol.* 22: 256–264.

Li, Z., Wang, S., Cheng, J., Su, C., Zhong, S., Liu, Q., et al. (2016b) Intron lariat RNA inhibits microRNA biogenesis by sequestering the dicing complex in Arabidopsis. *PLoS Genet.* 12: e1006422.

Lin, Y.C., Li, W., Chen, H., Li, Q., Sun, Y.H., Shi, R., et al. (2014) A simple improved-throughput xylem protoplast system for studying wood formation. *Nat. Protoc.* 9: 2194–2205.

Lu, T., Cui, L., Zhou, Y., Zhu, C., Fan, D., Gong, H., et al. (2015) Transcriptome-wide investigation of circular RNAs in rice. *RNA* 21: 2076–2087.

Maere, S., Heymans, K. and Kuiper, M. (2005) BiNGO: a cytoscape plugin to assess overrepresentation of gene ontology categories in biological networks. *Bioinformatics* 21: 3448–3449.

Matranga, C. and Zamore, P.D. (2007) Small silencing RNAs. *Curr. Biol.* 17: R789–R793.

Memczak, S., Jens, M., Elefsinioti, A., Torti, F., Krueger, J., Rybak, A., et al. (2013) Circular RNAs are a large class of animal RNAs with regulatory potency. *Nature* 495: 333–338.

Meng, X., Chen, Q., Zhang, P. and Chen, M. (2017) CircPro: an integrated tool for the identification of circRNAs with protein-coding potential. *Bioinformatics* 33: 3314–3316.

Ohashi-Ito, K. and Bergmann, D.C. (2006) Arabidopsis FAMA controls the final proliferation/differentiation switch during stomatal development. *Plant Cell* 18: 2493–2505.

Ostlund, G., Schmitt, T., Forslund, K., Kostler, T., Messina, D.N., Roopra, S., et al. (2010) InParanoid 7: new algorithms and tools for eukaryotic orthology analysis. *Nucleic Acids Res*. 38: D196–D203.

Pamudurti, N.R., Bartok, O., Jens, M., Ashwal-Fluss, R., Stottmeister, C., Ruhe, L., et al. (2017) Translation of circRNAs. *Mol. Cell*. 66: 9–21.e7.

Peng, Z., Zhang, C., Zhang, Y., Hu, T., Mu, S., Li, X., et al. (2013) Transcriptome sequencing and analysis of the fast growing shoots of moso bamboo (*Phyllostachys edulis*). *PLoS One* 8: e78944.

Peng, Z.H., Lu, Y., Li, L.B., Zhao, Q., Feng, Q., Gao, Z.M., et al. (2013) The draft genome of the fast-growing non-timber forest species moso bamboo (*Phyllostachys heterocycla*). *Nat. Genet*. 45: 456–461.

Pohl, M., Bortfeldt, R.H., Grutzmann, K. and Schuster, S. (2013) Alternative splicing of mutually exclusive exons—a review. *Biosystems* 114: 31–38.

Robinson, M.D., McCarthy, D.J. and Smyth, G.K. (2010) edgeR: a bioconductor package for differential expression analysis of digital gene expression data. *Bioinformatics* 26: 139–140.

Salzman, J., Chen, R.E., Olsen, M.N., Wang, P.L. and Brown, P.O. (2013) Cell-type specific features of circular RNA expression. *PLoS Genet.* 9: e1003777.

Salzman, J., Gawad, C., Wang, P.L., Lacayo, N. and Brown, P.O. (2012) Circular RNAs are the predominant transcript isoform from hundreds of human genes in diverse cell types. *PLoS One* 7: e30733.

Sanger, H.L., Klotz, G., Riesner, D., Gross, H.J. and Kleinschmidt, A.K. (1976) Viroids are single-stranded covalently closed circular RNA molecules existing as highly base-paired rod-like structures. *Proc. Natl. Acad. Sci. USA* 73: 3852–3856.

Schnable, P.S., Ware, D., Fulton, R.S., Stein, J.C., Wei, F., Pasternak, S., et al. (2009) The B73 maize genome: complexity, diversity, and dynamics. *Science* 326: 1112–1115.

Secco, D., Jabnoune, M., Walker, H., Shou, H., Wu, P., Poirier, Y., et al. (2013) Spatio-temporal transcript profiling of rice roots and shoots in response to phosphate starvation and recovery. *Plant Cell* 25: 4285–4304.

Shaikhali, J., Davoine, C., Brannstrom, K., Rouhier, N., Bygdell, J., Bjorklund, S., et al. (2015) Biochemical and redox characterization of the mediator complex and its associated transcription factor GeBPL, a GLABROUS1 enhancer binding protein. *Biochem. J.* 468: 385–400.

Shen, S.H., Park, J.W., Lu, Z.X., Lin, L., Henry, M.D., Wu, Y.N., et al. (2014) rMATS: Robust and flexible detection of differential alternative splicing from replicate RNA-Seq data. *P Natl Acad Sci USA* 111: E5593–E5601.

Trapnell, C., Roberts, A., Goff, L., Pertea, G., Kim, D., Kelley, D.R., et al. (2012) Differential gene and transcript expression analysis of RNA-seq experiments with TopHat and Cufflinks. *Nat Protoc* 7: 562–578.

Trapnell, C., Pachter, L. and Salzberg, S.L. (2009) TopHat: discovering splice junctions with RNA-Seq. *Bioinformatics* 25: 1105–1111.

Vazquez, F., Gasciolli, V., Crete, P. and Vaucheret, H. (2004) The nuclear dsRNA binding protein HYL1 is required for microRNA accumulation and plant development, but not posttranscriptional transgene silencing. *Curr. Biol*. 14: 346–351.

Wang, B.-B. and Brendel, V. (2004) The ASRG database: identification and survey of *Arabidopsis thaliana* genes involved in pre-mRNA splicing. *Genome Biol*. 5: R102.

Wang, H., Wang, H., Zhang, H., Liu, S., Wang, Y., Gao, Y., et al. (2019) The interplay between microRNA and alternative splicing of linear and circular RNAs in eleven plant species. *Bioinformatics*, https://doi.org/10.1093/bioinformatics/btz038.

Wang, J.W., Czech, B. and Weigel, D. (2009) miR156-regulated SPL transcription factors define an endogenous flowering pathway in *Arabidopsis thaliana*. *Cell* 138: 738–749.

Wang, T.T., Wang, H.Y., Cai, D.W., Gao, Y.B., Zhang, H.X., Wang, Y.S., et al. (2017) Comprehensive profiling of rhizome-associated alternative splicing and alternative polyadenylation in moso bamboo (*Phyllostachys edulis*). *Plant J.* 91: 684–699.

Werner, A.K., Medina-Escobar, N., Zulawski, M., Sparkes, I.A., Cao, F.Q. and Witte, C.P. (2013) The ureide-degrading reactions of purine ring catabolism employ three amidohydrolases and one aminohydrolase in Arabidopsis, soybean, and Rice. *Plant Physiol*. 163: 672–681.

Wu, B., Suo, F.M., Lei, W.J. and Gu, L.F. (2014) Comprehensive analysis of alternative splicing in digitalis purpurea by strand-specific RNA-seq. *PLoS One* 9: e106001.

Yang, L., Liu, Z., Lu, F., Dong, A. and Huang, H. (2006) SERRATE is a novel nuclear regulator in primary microRNA processing in Arabidopsis. *Plant J.* 47: 841–850.

Yang, X., Liu, D., Liu, F., Wu, J., Zou, J., Xiao, X., et al. (2013) HTQC: a fast quality control toolkit for Illumina sequencing data. *BMC Bioinformatics.* 14: 33.

Yang, Y., Fan, X., Mao, M., Song, X., Wu, P., Zhang, Y., et al. (2017) Extensive translation of circular RNAs driven by N(6)-methyladenosine. *Cell Res.* 27: 626–641.

Ye, C.Y., Chen, L., Liu, C., Zhu, Q.H. and Fan, L. (2015) Widespread noncoding circular RNAs in plants. *New Phytol.* 208: 88–95.

Ye, J., Zhang, Y., Cui, H., Liu, J., Wu, Y., Cheng, Y., et al. (2018) WEGO 2.0: a web tool for analyzing and plotting GO annotations, 2018 update. *Nucleic Acids Res.* 46: W71–W75.

Yokthongwattana, C., Bucher, E., Čaikovski, M., Vaillant, I., Nicolet, J., Scheid, O.M., et al. (2010) MOM1 and Pol-IV/V interactions regulate the intensity and specificity of transcriptional gene silencing. *EMBO J.* 29: 340–351.

Yu, Z.X., Wang, L.J., Zhao, B., Shan, C.M., Zhang, Y.H., Chen, D.F., et al. (2015) Progressive regulation of sesquiterpene biosynthesis in Arabidopsis and patchouli (*Pogostemon cablin*) by the miR156-targeted SPL transcription factors. *Mol. Plant* 8: 98–110.

Zhang, H., Lin, C. and Gu, L. (2017) Light regulation of alternative pre-mRNA splicing in plants. *Photochem. Photobiol.* 93: 159–165.

Zhang, H.X., Wang, H.H., Zhu, Q., Gao, Y.B., Wang, H.Y., Zhao, L.Z., et al. (2018) Transcriptome characterization of moso bamboo (*Phyllostachys edulis*) seedlings in response to exogenous gibberellin applications. *BMC Plant Biol*. 18: 125.

Zhang, X.O., Dong, R., Zhang, Y., Zhang, J.L., Luo, Z., Zhang, J., et al. (2016) Diverse alternative back-splicing and alternative splicing landscape of circular RNAs. *Genome Res.* 26: 1277–1287.

Zhang, X.O., Wang, H.-B., Zhang, Y., Lu, X., Chen, L.-L. and Yang, L. (2014) Complementary sequence-mediated exon circularization. *Cell* 159: 134–147.

Zhang, Y., Su, J., Duan, S., Ao, Y., Dai, J., Liu, J., et al. (2011) A highly efficient rice green tissue protoplast system for transient gene expression and studying light/chloroplast-related processes. *Plant Methods* 7: 30.

Zhang, Y., Zhang, X.O., Chen, T., Xiang, J.F., Yin, Q.F., Xing, Y.H., et al. (2013) Circular intronic long noncoding RNAs. *Mol. Cell.* 51: 792–806.

Zhao, T., Wang, L., Li, S., Xu, M., Guan, X. and Zhou, B. (2017) Characterization of conserved circular RNA in polyploid Gossypium species and their ancestors. *FEBS Lett.* 591: 3660–3669.

Zhou, M., Gu, L., Li, P., Song, X., Wei, L., CHen, Z., et al. (2010) Degradome sequencing reveals endogenous small RNA targets in rice (*Oryza sativa* L. ssp. indica). *Front. Biol.* 5: 67–90.

Zuo, J., Wang, Q., Zhu, B., Luo, Y. and Gao, L. (2016) Deciphering the roles of circRNAs on chilling injury in tomato. *Biochem. Biophys. Res. Commun*. 479: 132–138.